Magnetism in high-temperature superconducting compounds

Yu. A. Izyumov, N. M. Plakida, Yu. N. Skryabin

Institute of Physics of Metals, Urals Division, Academy of Sciences of the USSR, Sverdlovsk and Joint Institute for Nuclear Research, Dubna

Usp. Fiz. Nauk. **159**, 621–663 (December 1989)

Experimental data on the magnetic properties of copper oxide high-temperature superconductors (HTSCs) and their theoretical interpretation in terms of existing models are systematically reviewed. The crystal structure of the four existing classes of HTSCs (lanthanum, yttrium-barium, bismuth, and thallium) is described, and their band structure is analyzed on the basis of their crystal chemistry. The T, x and T, δ phase diagrams are reproduced for the well-studied compounds ($La_{2-x}Sr_xCuO_4$ and $YBa_2Cu_3O_{7-\delta}$). The magnetic structure of these compounds and their evolution with increasing concentration of impurities (x) and oxygen vacancies (δ) are analyzed. Data on the inelastic magnetic scattering of neutrons is discussed in detail, and it is shown that both compounds are quasi-two-dimensional antiferromagnets with spin 1/2. For values of x and δ for which there is no long-range magnetic order, both compounds exhibit two-dimensional antiferromagnetic correlations on the CuO_2 planes and high-energy spin excitations. This type of state is described as a "quantum spin fluid". The excitations may be the carriers of the pairing interaction between electrons in HTSCs. Basic theoretical models used to describe the physical properties of HTSCs are presented, including the two-dimensional Heisenberg model with spin 1/2, the nonlinear σ-model, and the Hubbard model with strong electron correlation near the half-filled state. Antiferromagnetism in HTSC compounds and its disappearance with increasing x or δ can be understood in terms of these models. The fundamentals of Anderson's theory of resonating valence bonds are presented together with his attempt to use it to explain the physical properties of copper oxide HTSCs in terms of neutral fermions (spinons) and charged bosons (holons). Alternative mechanisms are also discussed for electron pairing by magnetic fluctuations near the phase transition point with the formation of spin density waves. These mechanisms are based on the fact that the Fermi surface may be unstable near the half-filled state with respect to the formation of a dielectric state with a spin density wave. It is concluded that currently available experimental data on the magnetic properties of the HTSCs, and also other experimental data, cannot as yet be used as a basis for choosing between existing theories of high-temperature superconductivity. Nevertheless, many of the magnetic properties of copper oxides in their normal phase are satisfactorily interpreted by these theories.

1. Introduction. The past two years of intensive experimental research into the properties of copper oxide high-temperature superconductors (HTSCs) have demonstrated their exceptional physico-chemical complexity. The physical properties of all the existing classes of high-temperature superconductors are exceedingly sensitive to deviations from the stoichiometric composition, especially deviations due to doping or with divalent metallic elements or due to oxygen vacancies. A change in the impurity or vacancy concentration between relatively narrow limits is found to be accompanied by a whole series of phase transitions, so that the phase diagram on the temperature-concentration plane takes the form of a set of successive states, i.e., dielectric, metallic (normal and superconducting), and magnetically ordered states. Phase transitions between them have superimposed upon them transitions from the tetragonal to the orthorhombic phase. The superconducting state is thus seen to arise when the metal-dielectric and antiferromagnet-paramagnet transitions are close to one another. This means that any acceptable explanation of the HTSCs must be based on a study of the physical properties of not only the superconducting phase, but also of all the neighboring states on the phase diagram.

Luckily, there are many HTSCs, so that certain general properties can be identified by comparing the properties of the individual compounds. For example, it has been found that the charge carriers in all these compounds are holes in the copper oxide sublattice,[1] which are due to doping to oxygen vacancies. All the compounds exhibit strong anisotropy of electronic properties, e.g., electrical conductivity, which differs by several orders of magnitude in the direction of the c axis and in the a, b plane. Finally, we note the existence of three-dimensional antiferromagnetic order in compounds with stoichiometric composition or small deviations from it. Analysis of a large volume of experimental data on HTSCs has shown[1,2] that, despite the considerable anisotropy of many of their properties in the normal phase, superconductivity is more likely to have a three-dimensional character, and the correlation lengths ξ in the direction of the principal axis of the crystal and along the CuO_2 planes differ by a factor of only several units.

Extensive fundamental experimental data, including observations of the Knight shift below T_c, show that the singlet Cooper pairing of carriers occurs in open HTSCs, but the mechanism responsible for this pairing, which leads to such high T_c for the superconducting transition, is still not understood. The traditional phonon mechanism encounters serious difficulties when an attempt is made to use it to explain the properties of the HTSCs. They include the weak isotopic effect, the high T_c, and the contradictory data on strong electron-phonon coupling. At the same time, even the early work on the HTSCs had already revealed the remark-

 0038-5670/89/121060-24$01.80

able magnetic properties of the lanthanum and yttrium-barium systems. These properties were subsequently discovered in other HTSCs as well. They include antiferromagnetic order in the copper sublattice near compositions for which superconductivity is found to occur, and strong fluctuations in the magnetic order parameter at temperatures above the Néel point, or for compositions for which there is no long-range magnetic order. These fluctuations have a well-defined quasi-two-dimensional character, and their anomalously high intrinsic energy is of the order of the electron energies. All this has led to the hypothesis that electron pairing in copper oxide compounds can proceed via the magnetic degrees of freedom, and has acted as a considerable stimulus to theoretical research.

The aim of this review is to examine the magnetic properties of copper oxide HTSCs and, especially, to present a systematic summary of existing experimental results. Our review is therefore complementary to the recent survey of experimental studies given by Gor'kov and Kopnin.[1] A systematic account of experimental data on magnetic structure and spin dynamics must rely on fundamental data on the crystal structure, crystal chemistry, and the electronic structure of the HTSCs. These data are now well established and can serve as reference material for future publications in this journal on high-temperature superconductivity.

The theory of these magnetic properties has had two aims, namely, to explain the magnetic behavior of the compounds, which is particularly well-defined for compositions for which the compounds are not superconducting, and, secondly, to examine the possibility of electron pairing through the magnetic excitation of the system, i.e., to search for possible mechanisms of HTSC. The theoretical part of our review is largely confined to the former aspect, since none of the many theoretical models of HTSC has been unambiguously verified by experiment.

I. Basic experimental data

2. Crystal structure. The four known classes of high-temperature superconductors have different crystal structures, but, nevertheless, have much in common with each other. Common features include the existence of square CuO_2 planes that alternate with planes consisting of other metallic elements and constantly repeat the same motif: the Cu atoms are in the octahedral environment of the O atoms and form the CuO_6 complexes or complexes with oxygen vacancies (CuO_5 and CuO_4). We begin with a brief description of the basic structures of HTSCs.

La_2CuO_4 is found to be in the tetragonal phase at high temperatures (space group $I4/mmm$—D_{4h}^{17}), whereas at low temperatures it is found in the orthorhombic group ($Cmca$—D_{2h}^{18}). This is the K_2NiF_4 type structure: each Cu atom is surrounded by an O_6 octahedron.

A phase transition to the ortho phase occurs at a certain temperature T_0 and is due to the rotation of the central octahedron around the [110] direction and out-of-phase rotations of octahedra in neighboring cells. This structural transition is a classic phase transition that occurs in accordance with the soft-mode mechanism observed in many perovskites.[3,4]

The typical lattice constants in the tetra and ortho-phases are ($a_t = 3.7873$ Å, $c_t = 13.2883$ Å, $a_0 = 5.3562$ Å, $b_0 = 5.3990$ Å, $c_0 = 13.1669$ Å) for compositions containing a small amount of Ba instead of La (Ref. 3). As can be seen, the system is only slightly orthorhombic, so that

$$a_0 \approx b_0 \approx \sqrt{2}\, a_t.$$

The separations between the oxygen and copper atoms in a plane and along the z axis are as follows: 1.8936 Å (Cu—O1) and 2.428 Å (Cu—O2).

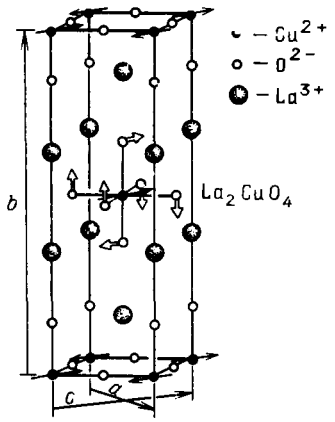

FIG. 1. The crystal structure of La_2CuO_4. Arrows show the displacement of the oxygen atoms in the orthorhombic phase.

Nonstoichiometric compounds of the form $La_{2-x}M_xCuO_{4-\delta}$ that contain small amount of a divalent metal (M = Sr, Ba, Ca), and oxygen vacancies with the composition $La_{2-x}M_xCuO_{4-\delta}$, have a similar structure. The temperature T_0 decreases with increasing dopant concentration. Figure 2 shows a typical phase diagram in the x, T plane.

The second famous class of high-temperature superconductors has the form $YBa_2Cu_3O_{7-\delta}$. As in the case of La_2CuO_4, the unit cell looks like a set of three cubic perovskite cells, one on top of another. The structure depends on the concentration of oxygen vacancies, i.e., the parameter δ. When $\delta = 0$, we have the orthorhombic structure $Pmmm$—D_{2h}^1. The unit cell is shown in Fig. 3 and contains one formula unit. The copper atoms in this structure form the CuO_2 planes and CuO chains running along the b direc-

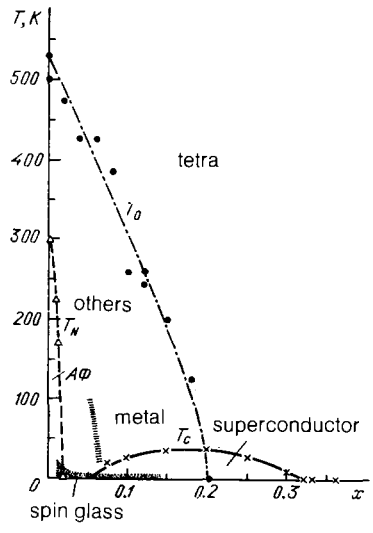

FIG. 2. Phase diagram for $La_{2-x}Sr_xCuO_4$ (Ref. 27).

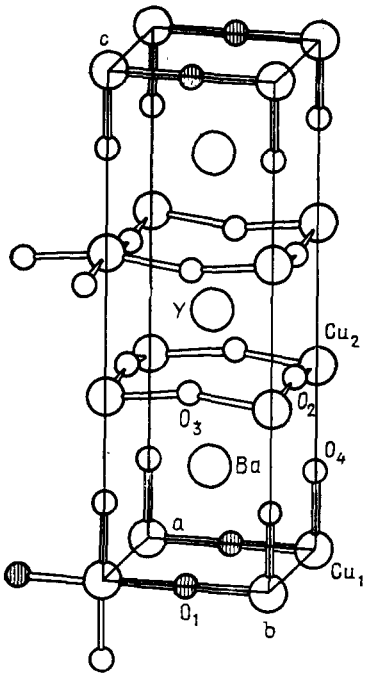

FIG. 3. Unit cell of $YBa_2Cu_3O_{7-\delta}$ in the orthorhombic phase.[5]

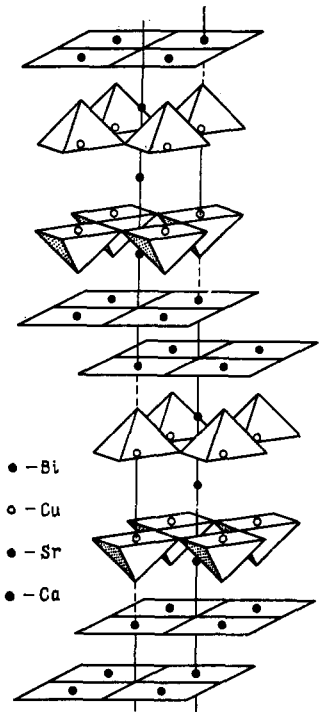

FIG. 4. Unit cell of $Bi_2Sr_2CaCu_2O_8$.

tion. The Cu atoms in the planes are surrounded by five O atoms forming the CuO_5 group, i.e., an incomplete octahedron (pyramid). The unit-cell parameters depend on δ and on the temperature. Thus, when $\delta = 0.09$ and $T = 95$ K) we have the following parameter values and separations between the nearest-neighbor Cu and O (Ref. 6): $a = 3.8099$ Å, $b = 3.8789$ Å, $c = 11.6425$ Å; Cu1—O1: 1.941 Å, Cu1—O4: 1.957 Å; Cu2—O2: 1.925 Å; Cu2—O3: 1.957 Å; and Cu2—O4: 2.777 Å.

It is clear that the Cu–O bond lengths for the nearest four O atoms in planes and chains are roughly equal and that there are long Cu–O bonds in planes for La_2CuO_4. The Cu2—O_4 separation in the Cu–O5 pyramid is shorter than the corresponding distance along the z axis in La_2CuO_4, which may play a definite part in strengthening the bonding between the planes in Y–Ba compounds as compared with La_2CuO_4.

Structural studies show that thermal factors are highly anisotropic, especially for the O atoms in chains, in directions perpendicular to them. There are experimental[6] and theoretical [7] reasons for supposing that these atoms are in double-well potentials and are randomly distributed over two positions at a distance of the order of ± 0.1 Å from the chain axis in the direction of the a axis.

Heating above 700 °C produces a transition from the ortho to the tetra phase as a result of the formation of oxygen vacancies in chains in $(0\ \frac{1}{2}\ 0)$ positions and the filling by them of the free $(\frac{1}{2}\ 0\ 0)$ positions. Equalization of oxygen concentration in these positions produces the tetragonal structure $P4/mmm$—D^1_{4h}. The O→T transition is also observed as a consequence of substitution by the rare earths Nd, Sm Eu, Gd, and Dy (Ref. 8). The electron microscope has revealed twinning as $T \to 0$ and the formation of a system of orthorhombic domains of the form (110) and $(1\bar{1}0)$ (Ref. 9). It has also been found that the oxygen vacancies form a superlattice whose period varies with the concentration δ (Ref. 10).

A still more complicated structure is revealed by new classes of HTSCs based on bismuth and thallium, but containing no rare earth ions. Figure 4 shows the unit cells of the Bi compound investigated in the case of the single crystal $Bi_{2.2}Sr_2Ca_{0.8}O_{8+\delta}$ with $T_c = 84$ K and the following lattice constants:[11] ($a = 5.414$ Å, $b = 5.418$ Å, $c = 30.89$ Å. The unit cell contains one formula unit (space group $Fmmm$). As in the case of the Y–Ba compound, the structure consists of CuO_5 pyramids (the Cu—O distance in a plane is ~1.9 A and the Cu—O2 distance along the z axis ~2.2 Å). However, in contrast to $YBa_2Cu_3O_{7-\delta}$, this compound does not contain Cu—O chains: their role is replaced with Bi_2O_2 double layer with the NaCl structure. The main phase in this compound is chosen in Ref. 12 to be the tetragonal phase $I4/mmm$ with unit cell parameters $a_t = b_t = 3.814$ Å $c_t = 30.52$ Å, related to the orthorhombic cell by

$$a \approx b \approx \sqrt{2}a_t.$$

In addition to the orthorhombic distortion of this pseudotetragonal structure there is also an incommeasurate modulation with a small amplitude, probably in the Bi_2O_2 plane.

Further analysis has demonstrated the possible existence of structures with a large number of CuO_2 planes, separated by Ca ions, with the general formula $A_2B_2Ca_{n-1}Cu_nO_{4+2n}$, where A = Bi, Tl and B = Sr, Ba for $n = 1, 2, 3$. The thallium structure with $n = 2$ differs by the fact that the CuO_5 pyramid is much more distorted: the Cu—O1 separation in a plane is ~1.92 Å, and the Cu—O2 separation along the z axis is ~2.70 Å. The additional CuO_2 plane that appears in the structure with $n = 3$ does not have a significant effect on the principal parameters of the unit cell, and only increases the constant along the z axis by about 5 Å.

3. Doping and superconductivity. Superconductivity arises in copper oxide compounds when there is a deviation from the stoichiometric composition due to the replacement

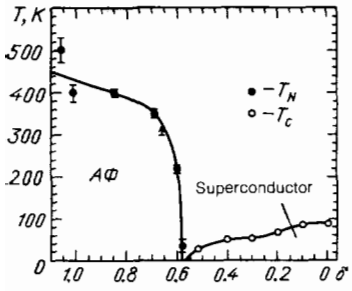

FIG. 5. Phase diagram for $YBa_2Cu_3O_{7-\delta}$ (Ref. 13).

of metallic elements, or there is a change in the oxygen content. Figure 2 shows that superconductivity appears in the lanthanum system when La^{3+} ions in La_2CuO_4 are replaced with the divalent ions Sr^{2+}. Doping with other divalent metals, for example, Ba and Ca, produces a similar effect. On the other hand, in the yttrium-barium system, superconductivity arises $YBa_2Cu_3O_{7-\delta}$ only when the concentration δ of oxygen vacancies is low enough (Fig. 5). When $\delta \lesssim 1$, the crystal structure is tetragonal and contains the dielectric and magnetically ordered phases, but for $\delta < 0.6$, the structure is orthorhombic and the superconducting phase appears.

The maximum T_c is achieved in $La_{2-x}Sr_xCuO_4$ for $x = 0.15$ ($T_c \approx 40$ K). The replacement of copper with the divalent ions of 3*d*-metals, i.e., Ni,Fe, Co, etc, and also Zn, leads to the rapid suppression of superconductivity. Whereas in the case of Ni, Fe, and Co the phenomenon can be explained in terms of the effect on electron pairing, of scattering by the localized magnetic moment the suppression by the Zn impurity is unexpected.

A more complicated effect of copper-replacing impurities is observed in $YBa_2Cu_3O_{7-\delta}$, and also in isomorphic compounds in which Y is replaced with a rare-earth metal. The suppression of T_c by impurities in the form of different 3*d*-elements is illustrated in Fig. 6 from which it is clear that T_c anticorrelates with the magnetic susceptibility $\chi(T)$ that is largely due to impurities introduced into the medium.[14] If the valley on the $T_c(n)$ curve is due to the paramagnetic Fe, Co, and Li impurities, the sharp reduction in T_c due to the

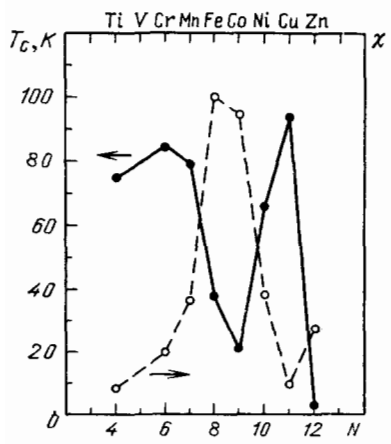

FIG. 6. Superconducting transition temperature and magnetic susceptibility of $YBa_2(Cu_{0.9}M_{0.1})_3O_{7-\delta}$ doped with 3*d*-elements.[14] *N* is the number of valence electrons in the impurity atom.

Zn impurity (as in the La-Sr system) is also unexpected. The fact that, even for this high concentration of the magnetic impurity (about 10%), the superconductivity is still not suppressed, suggests that the oxide superconductors have unusual properties whereby even a nonmagnetic impurity can produce a considerable suppression of T_c.

The type of substituent position was not examined in Ref. 15, but particular attention was paid in Ref. 15 to the position of the substituent (Cu2 or Cu1). The two systems $YBa_2(Cu_{1-x}Zn_x)_3O_7$ and $YBa_2(Cu_{1-x}Ca_x)_3O_7$, with Zn and Ga impurities, whose ionic radii were close to the ionic radius of Cu, were investigated. Neutron diffraction data show that Zn replaces Cu mostly in planes, whereas Ga replaces them in chains, so that it is interesting to compare the effect of doping on T_c in both cases. It is found that the Zn^{2+} impurities rapidly suppress superconductivity without affecting the orthorhombic phase. On the other hand, Ga^{3+}, which replaces copper in chains has very little effect on T_c, but even a small concentration ($\sim 6\%$) produces a phase transition to the tetragonal phase. On the other hand, in the normal phase, the resistance increases by a factor of several units when the Ga impurity is introduced. It follows that the CuO_2 planes and not the CuO chains play the main role in the onset of HTSC. This is confirmed indirectly by the rapid suppression of superconductivity in $La_{2-x}Sr_xCuO_4$ by a small concentration ($\sim 2.5\%$) of Zn or Ga. This compound has only one copper position (in the CuO_2 plane), so that the Zn and Ga impurities produce a comparably strong suppression of T_c.

We therefore conclude that the CuO_2 planes play the dominant part in the onset of HTSC in the La–Sr and Y–Ba compounds. The structure of the lattice (tetragonal or orthorhombic) does not play a significant part in this. The superconducting phase can be produced in the tetragonal structure by introducing a suitably chosen dopant. The dominant role of the CuO_2 planes is also confirmed by the discovery of the bismuth and thallium HTSC in which the copper ions are confined to the CuO_2 planes.

4. *Crystal chemistry and electronic structure.* Band structure calculations and x-ray and optical spectroscopy show that the metallic properties of copper oxide HTSCs are largely determined by the interaction between the outer-shell electrons of Cu and O, whereas the other ions have well-localized charges and form the ionic skeleton of the lattice. The principal structural element of all known HTSCs is the CuO_2 plane. Each Cu ion on this plane is at the center of a CuO_6 octahedron in the La compounds, or an incomplete CuO_5 octahedron (pyramid) in the Y or Bi compounds.

The five-fold degenerate atomic *d*-level of the Cu ion

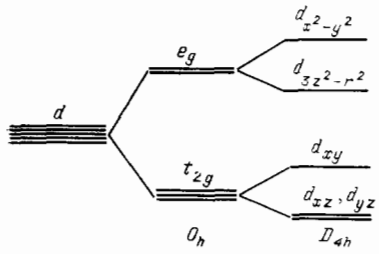

FIG. 7. The *d*-level splitting in the crystal field of cubic and tetragonal symmetry.

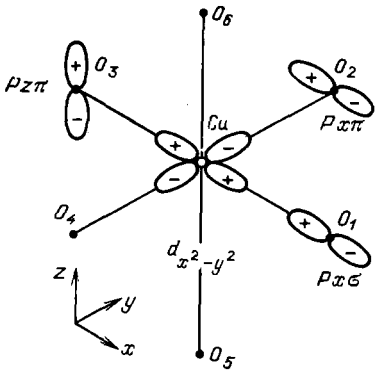

FIG. 8. Orbitals on Cu and O ions in the CuO_6 octahedron.

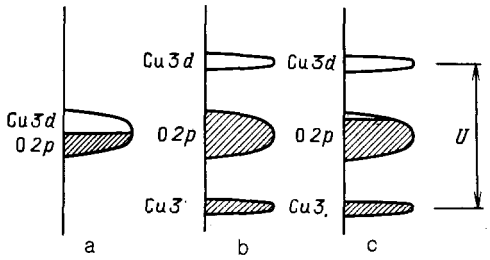

FIG. 9. Model electron structure of the copper oxides:[18] a—half-filled $3d$-$2p$-band without Coulomb correlations, b—ditto, but including strong d-d Coulomb correlation, c—metallic state as the number of holes in the CuO system increases. The bottom structures in Figs. b and c correspond to Cu$3d$.

splits in a field of cubic symmetry into two two-fold and three-fold degenerate levels e_g and t_{2g}, and an additional splitting occurs in a tetragonal field (Fig. 7). Typically, the separation between the levels e_g and t_{2g} is about 1 eV, and the splitting of e_g in a field of tetragonal symmetry is about 0.7 eV (Ref. 16). This splitting is due to the elongation of the oxygen octahedron in the HTSC structure, and also the Jahn-Teller effect.

If we look upon the state Cu^{2+} ($3d^9$) as a hole in the filled $3d$-shell of copper, we find in accordance with Fig. 7 that the hole should lie in the upper unfilled $d_{x^2-y^2}$ level. The three-fold degenerate p-level of oxygen splits into the singlet p_z and doublet (p_x,p_y) in a field of tetragonal symmetry.

Figure 8 shows the CuO_6, complex taken from the CuO_2 plane. The $d_{x^2-y^2}$ orbital of the hole is shown on the copper ion and the p_x,p_y, and p_z orbitals on the oxygen ions. Only one orbital per oxygen ion is indicated for the sake of simplicity. In the crystal, the p-orbitals are given an additional designation in order to show their orientation along the direction joining a given O to ion to the Cu ion. Thus, p-orbitals lying along this direction are called σ-orbitals, whereas those perpendicular to it are known as π-orbitals. The interaction between all these orbitals in the Cu and O ions forming the CuO_2 plane determines the energy spectrum of electrons in this plane. This often assumes (see for example, Ref. 16) that the p-holes in the π-orbitals have the lowest energy because the splitting in the crystal field of the ionic skeleton of the lattice is then smaller than for states on the σ-orbitals. It may therefore be expected that new holes that appear in the CuO_2 plane as a result of doping are mostly localized in the p-bands of oxygen, constructed from π-type orbitals. The $d_{x^2-y^2}$ and ($p_{x\sigma}$,$p_{y\sigma}$) orbitals are the most strongly bonded, and this leads to a wide band of $dp\sigma$-states when the electron band structure is calculated. The ($p_{x\pi}$,$p_{y\pi}$) and $p_{z\pi}$ orbitals that do not interact with the $d_{x^2-y^2}$ and $d_{3z^2-r^2}$ states of Cu form an individual π-band because of the direct overlap of the p_π-orbitals and also because of indirect coupling via the $d_{xy}d_{yz}d_{xz}$ orbitals of Cu. This model also predicts two effective subbands (σ and π) that are weakly coupled to one another. In the $|3d^9 2p^6\rangle$ state, the holes are located in the half-filled σ-band, and the new holes appear mostly in the $|2p^5\rangle$ π-band of oxygen.

Let us examine in greater detail this system of hole levels in the crystal field, taking into account Coulomb correlation on a single copper ion. In the $3d$-state of Cu, this energy is relatively low: $U_d \approx 7$–8 eV. When the single-site Coulomb interaction is taken into account, the filling of the $3d$-levels of Cu becomes more complicated. If in the Cu^{2+} ($3d^9$) state there is one $d_{x^2-y^2}$ hole in the ε_d level, the second hole (the $3d^8$ state) can appear only in the level with energy $\varepsilon_d + U_d$. Such a high Coulomb correlation energy, exceeding the width W of the d-band ($U_d > W$), ensures that the copper oxides in which copper is in the Cu^{2+} state, and there is one hole per primitive cell, are Mott-Hubbard dielectrics.[17] The observed finite conductivity is then typical of a semiconductor ($d\rho/dt < 0$) and is due to the presence of impurity carriers. These compounds can assume the metallic state with hole-type conductivity if we increase the number of holes by altering the concentration x and also the concentration of oxygen in the La and Y compounds. It is clear from the foregoing that additional holes are probably formed in the p-orbitals of the $2p^6$ states of oxygen. Figure 9 illustrates these qualitative ideas about the electron structure of copper oxide compounds in terms of single-ion orbitals.

This crystal chemistry analysis must be compared with band structure calculations. The very first calculations[19,20] performed by the method of linearized plane waves, showed that the main contribution to the electron density of states near the Fermi surface of La_2CuO_4 was provided by the $pd\sigma$-band constructed from $d_{x^2-y^2}$ states on Cu^{2+} and $p_\sigma(x)$,$p_\sigma(y)$-states on O^{2-} (Fig. 10). Of the seventeen bands formed from the Cu($3d$)—O($2p$)-states (five $3d$-states on the Cu ion and three $2p$-states on the four O ions in a unit cell of the crystal), only two bands have high dispersion. They are the so-called bonding band (B) and antibonding band (A). The Fermi surface intersects an A-type band and the remaining bands lie well below the Fermi energy. Since electrons in the $pd\sigma$-band are localized in the CuO_2 planes lying at a considerable distance from one another, this band is essentially two-dimensional, i.e., the dispersion along the axis is small [cf. the line Λ drawn between the center of the band Γ and the point Z (0 0 1/2). The La levels are weakly coupled to the states in the Cu—O bands: the $5d$-level of La lies 1 eV above the $5p$-level 15 eV below the Fermi level. We can therefore regard La as an isolated ion whose replacement with a rare-earth element with an equal charge has little effect on electronic properties. In particular, there is little magnetic scattering of electrons into the $pd\sigma$-bands, by the magnetic moment of rare-earth ions, and superconductivity is not suppressed thereby.

The two-band approximation to the spectrum in the strong coupling approximation[19] is meaningful because of the two-dimensional character of bands near the Fermi sur-

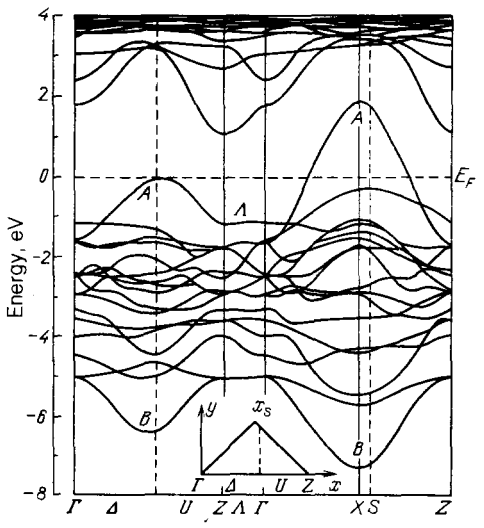

FIG. 10. Bands of electron energy states in the tetragonal phase of La_2CuO_4 (Ref. 19).

face. A hybridized p-d band on a CuO_2 plane is described by the formula

$$E_{A,B}(k) = \frac{1}{2}\left[(\varepsilon_p - \varepsilon_d)^2 + 4t^2\left(\sin^2\frac{k_x a}{2} + \sin^2\frac{k_y a}{2}\right)\right]^{1/2},$$

where $\varepsilon_p, \varepsilon_d$ are the atomic $2p$- and $3d$-states of Cu and O, and t is the matrix element of the transition between the nearest neighbors of Cu and O in the plane. Comparison with the calculated spectrum (Fig. 10) gives $\varepsilon_p \approx \varepsilon_d = -3.2$ eV, $= (t\sqrt{3}/2)V_{pd\sigma}, V_{pd\sigma} = -1.8$ eV. The total width of the A- and B-bands is

$$W = 4\sqrt{2}t \approx 9 \text{ eV}.$$

These data define the energy scale in the electron spectrum of La_2CuO_4 without taking into account the electron correlation on the copper ions.

The strong anisotropy of the $pd\sigma$-band leads to the quasi-two-dimensional character of the Fermi surface. In the strong coupling approximation for the half-filled A-band, the Fermi surface is determined by the condition $E_A(k_F) = 0$,

$$\sin^2\frac{k_x a}{2} + \sin^2\frac{k_y a}{2} = 1,$$

the solution of which is $|k_x| + |k_y| = \pi/a$. In Fig. 11 we show the Brillouin zone ($\pm \pi/a$, $\pm \pi/a$) of a square lattice and the Fermi surface in the form of the straight lines AB, BC, CD, and DA. The Fermi surface touches the Brillouin zone at the points A, B, C, and D, and this leads to the van Hove singularity in the density of electron states $N(\varepsilon)$. A more rigorous calculation[20] shows that this occurs in the doped compound $La_{2-x}M_xCuO_4$, where M = Sr, Ba for $x \approx 0.15$. Consequently, the Fermi surface for this concentration passes through the van Hove singularity, and $N(\varepsilon)$ has its maximum value. The maximum value of T_c is often associated with the latter.

On the other hand, the presence of flat segments on the Fermi surface ensures a high degree of congruence of this surface when it is displaced by $|\mathbf{q}_{1,2}| = 2k_F, \mathbf{q}_{1,2} = (\pi/a, \pm \pi/a, 0)$. Such a strong singularity usually leads

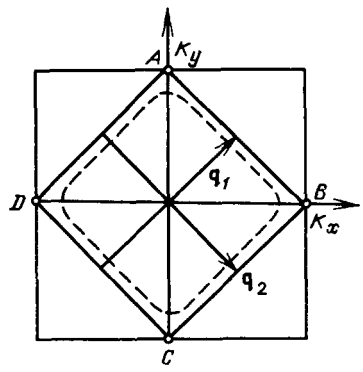

FIG. 11. Two-dimensional Fermi surface in the tetragonal phase of La_2CuO_4 (Ref. 19).

to an instability of the lattice and to the formation of charge density waves (CDW). However, the observed structural phase transition $D_{4h}^{17} \rightarrow D_{2h}^{18}$, due to an increase in the lattice period in the basal plane by the factor of $\sqrt{2}$, which in turn is due to the condensation of the soft lattice mode with wave vector $\mathbf{q}_1$ ($\mathbf{q}_2$), does not lead to the formation of the charge density wave. This transition is accompanied only by a change in the separation between the O ions in the basal plane, but the Cu—O separations remain the same for all four O ions, and there is no gap in the electron spectrum on the Fermi surface. The gap could have arisen during the freezing of the "breathing" mode associated with the motion of the oxygen ions in the basal plane along the Cu—O bonds. The absence of this type of structure, or transition with the freezing of the "breathing" mode, suggests that the band calculations of Refs. 19–21 did not satisfactorily reflect the real structure of the energy bands in La_2CuO_4. It would appear that the presence of strong Coulomb correlations in the $3d$-band of Cu produces a considerable reduction in the instability of this type of lattice without at the same time preventing the freezing of the rotational soft mode.

Another difficulty of the band theory of La_2CuO_4, which does not take electron correlations into account, has to do with the explanation of the dielectric state and antiferromagnetism. Since the unit cell contains one Cu atom, the $d_{x^2-y^2}$ band of copper states is half-filled, so that this compound should be a metal. All this points to the importance of many-particle effects (Coulomb correlation) in copper oxide HTSCs, which are ignored in the single-particle band theory. It is then legitimate to ask: is there any validity in the standard band calculations of the physical properties of these HTSCs? The answer must be in the affirmative. Band calculations provide us with useful information about the importance of the coupling between the e_g-states of Cu and the p-states of O in CuO_2 planes, the quasi-two-dimensional character of these states, the magnitudes of the electron transfer parameters t_l, t_d in the copper and oxygen sublattices, the parameter t_{dp} of transitions between sublattices, and so on. The most difficult question is the position of the Fermi level, since Coulomb correlation in the individual copper atoms splits the spin double degenerate level into two well-separated levels, so that the number of possible "target places" for the d-electrons (this determines the Fermi level) is substantially altered.

In the band theory employing the mean-field approximation, the Coulomb repulsion energy U between electrons

in an atom produces a shift of the atomic level ε_d by the amount $U\langle n_d\rangle$, so that, in the paramagnetic state, there is a d-band with energy $E_d(k) = \varepsilon_d(k) + U\langle n_d\rangle$ for both spin orientations. The necessary condition for the hybridization of the d-band and the p-electron band on the Fermi surface is $E_d(k) \approx \varepsilon_p(k)$. This is possible if the atomic level ε_d lies below the atomic level ε_t by an amount of the order of $U\langle n_d\rangle$. It is only then that we obtain the structure of the spectrum shown in Fig. 9, which is thought to be representative (at least qualitatively) of all classes of copper oxide HTSCs.

Band structure calculations have also been performed for other classes of HTSCs, i.e., for the Y, Bi, and Tl compounds (Refs. 22, 23, and 24, respectively). The structure of the spectra is qualitatively similar to that of the La system. The pd_6-hybridization of states on CuO_2 planes is found to occur throughout, and these planes emerge on the Fermi surface with a small density of states N(O). The states of other ions lie outside the limits of the Fermi surface, so that their replacement with others does not as yet produce a significant change in the electron properties of these compounds. Of course, the electron spectra exhibit some differences associated with details of their crystal structure, e.g., the existence of Cu—O chains in the Y system and of a large number of CuO_2 layers in the Bi and Tl systems. An interesting feature of the latter compounds is the presence of the "electron pockets" near the Fermi surface, which consist of the 6p- and 6s-states of Bi and Tl, respectively. The most topical and complex problem for the methods of calculation examined above[2] is how the band calculations could be modified so that the strong single-site Coulomb correlations could be taken into account.

An understanding of many of the properties of copper oxide HTSCs can be achieved on the basis of the simplified picture of the electron structure that follows from the crystal chemistry of these compounds, and by taking into account the comparable electron correlations. The magnetic properties of the HTSCs will in fact be treated from this point of view.

The paper of Anisimov *et al*[26] in which an attempt was made to take strong correlations into account in band calculations appeared after this review was practically complete. The idea was to allow for the difference between the potentials experienced by electrons in filled and unfilled states. The first stage of the method relies on standard band calculations without taking into account correlations, which determine the Fermi level. For electron states lying above the Fermi level, the potential is calculated with the electron configurations altered by one. This takes into account the correlation effect in the subsequent calculations. The procedure was used in a self-consistent calculation for La_2CuO_4. Figure 12 shows the calculated densities of states in the neighborhood of the Fermi level. The striking feature is the appearance of a gap at the Fermi level of the standard calculation without correlation. The compound La_2CuO_4 is therefore a dielectric with a band gap of 0.86 eV. More than that, in the ground state, it is an antiferromagnet with a magnetic moment of 0.38 μ_B per atom. All these data are in good agreement with experiment. We thus see two half-filled Hubbard bands. The rapid variation in the density of states near the band edges corresponds to the van Hove singularities of the

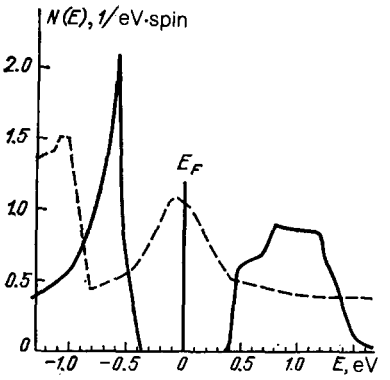

FIG. 12. Density of electron states in La_2CuO_4, calculated from first principles by a new method that takes electron correlations into account.[26] Dashed curve shows the usual band calculations.

two-dimensional spectrum corresponding to the CuO_2 plane. This band structure leads to a sharp change in the density of states at the Fermi level when holes are formed in the band, and this may explain the sensitivity of many of the properties to dopants in the form of divalent metals. The new method appears to provide a qualitative description of many of the physical properties of highly correlated systems such as all the copper oxide HTSCs.

5. *Magnetic structure.* Stoichiometric La_2CuO_4 is a collinear antiferromagnet with the Néel point[27-29] $T_N \approx 300$ K. It is clear that Fig. 1 that magnetic order occurs in the orthorhombic phase, and that the alignment of the magnetic moments of the copper ions is closely related to structural distortions in this phase. It is clear from Fig. 1 that the magnetic moments are oriented in the direction in which the oxygen atoms are displaced during the spontaneous rotation of the octahedra. The magnetic unit cell is the same as the orthorhombic cell whose parameter is greater by the factor $\sqrt{2}$ than the cell parameter in the tetragonal phase. Figure 13 shows the magnetic cell of La_2CuO_4 (only the copper atoms are indicated). The magnetic moment of a copper site is[29] $\mu \approx 0.5 \pm 0.15\mu_B$. The magnetic moment of the copper ion Cu^{2+} with spin $S = 1/2$ should be $\mu = gS\mu_B = 1.14\mu_B$. The observed smaller value of the magnetic moment may be

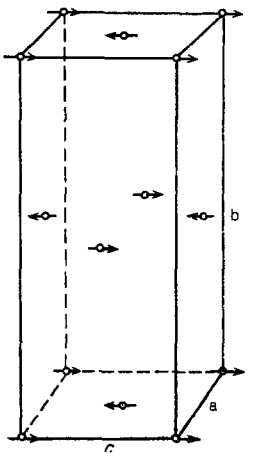

FIG. 13. Magnetic unit cell of La_2CuO_4 (Ref. 29).

due to quantum fluctuations and the influence of the covalent bond between Cu and the O ion.[27]

The interesting feature of the antiferromagnetic spin ordering in La_2CuO_4 is the weak ferromagnetic moment in the CuO_2 planes, which is perpendicular to them and has opposite directions involved in neighboring planes.[30,31] The ferromagnetic moment is $2\cdot 10^{-3}\mu_B$ per copper atom. It arises when the copper spins leave the a, c plane as they rotate by a small angle ($\sim 0.17°$) because of the rotation of the octahedra in the orthorhombic phase (cf. Fig. 1). The octahedra are in antiphase on neighboring planes, and this ensures that the ferromagnetic moments on neighboring planes have opposite directions. There is no doubt that structural distortions in the ortho phase and the magnetic ordering are symmetrically coupled. Symmetry analysis shows[32] that both phase transitions occur on a two-prong star of the wave vector (the point X) of the tetragonal body-centered original lattice.

T_N is found to be very sensitive to the concentration of oxygen vacancies that replace the divalent La (in the same way as the structural transition point[30] T_0) and also to the divalent metal impurities Sr and Ba. It is clear from Fig. 2 that for Sr concentrations $x \approx 0.02$, long range magnetic order is already almost completely destroyed. This cannot be understood in terms of the classical percolation model, and requires the inclusion of the effect of holes introduced by the impurity.[33]

Electric transport in these media is due to electron holes localized on oxygen ions.[18] Let us consider the instantaneous configuration with one hole on the O^- ion. The hole spin σ interacts via exchange forces with the two neighboring copper spins $\mathbf{S}_1$ and $\mathbf{S}_2$. The Hamiltonian for this interaction is

$$\mathcal{H} = -J_\sigma \sigma (\mathbf{S}_1 + \mathbf{S}_2) \qquad (5.1)$$

and it is intuitively clear that, whatever the sign of J_σ, the ground state should correspond to parallel spins $\mathbf{S}_1$ and $\mathbf{S}_2$. The interaction (5.1) must therefore give rise to an effective ferromagnetic interaction of the form $\mathcal{H}' = -K\,\mathbf{S}_1\mathbf{S}_2$ due to the holes. The strength K of this interaction should be comparable with the antiferromagnetic interaction J producing the antiferromagnetic order in La_2CuO_4. The competition between ferro- and antiferromagnetic interactions leads to the frustration of exchange bonding, the result of which is the long range magnetic order at a certain critical concentration, and the formation of the spin glass phase for a relatively wide range of values of x. Apart from the frustration mechanism, the destruction of antiferromagnetic order is also substantially influenced by the motion of holes because their delocalization produces a gain their kinetic energy. The compound $YBa_2Cu_3O_{7-\delta}$ with $\delta \lesssim 1$ (in the dielectric phase) exhibits antiferromagnetic ordering of magnetic moments on the Cu2 sites in CuO_2 planes,[27,34,35] which is completely analogous to antiferromagnetic ordering in La_2CuO_4. The volume of the magnetic cell is greater by a factor of 2 than the volume of the crystal cell, and its parameters on the basal plane are $\sqrt{2}a, \sqrt{2}a$, where a is the cell parameter in the tetragonal phase [the wave vector of the magnetic structure is (1/2, 1,2, 0); Fig. 14a]. The magnetic moments of the Cu1 ions in chains appear only for $\delta < 1$, and can be ordered at low enough temperature, as shown in Fig. 14b.

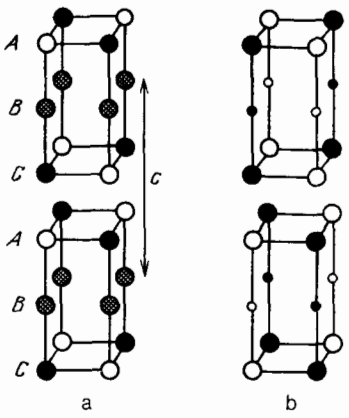

FIG. 14. Magnetic ordering in $YBa_2Cu_3O_{7-\delta}$ for $\delta \lesssim 1$: a—$\delta \approx 1$ (Ref. 34), b—$\delta < 0.9$ (Ref. 35). Copper atoms are indicated. Full points and open circles represent antiparallel orientation of spins, unrelated to any particular direction in the crystal. Shaded circles represent unordered magnetic atomic moments.

It is useful to note that lines containing copper ions correspond to bonding via oxygen atoms lying along these directions. There is no bonding between planes C and A because there is no oxygen atom at the apex of the octahedron for this structure (cf. Fig. 3), so that the bonding between them is assumed to be due to dipole forces.

It is clear from Fig. 5 that magnetic order is very dependent on the oxygen content. The figure shows the dependence of the temperatures of magnetic ordering and of the superconducting transition as functions of the concentration δ of oxygen vacancies. These data were deduced from neutron diffraction studies, but they agree with μSR data reported in Ref. 36.

The maximum temperature $T_N \approx 500$ K is greater than T_N for La_2CuO_4 by a factor of almost 2. This is probably due to the difference between the bonding of the CuO_2 planes in these two structures. In the Y–Ba system, exchange bonding between the copper ions is accomplished via the oxygen in accordance with the scheme Cu^{2+}—O—Cu^{2+} whereas, in the La-system, the indirect exchange chain is longer: Cu^{2+}—O^{2-}—La^{3+}—O^{2-}—Cu^{2+}. The other possible explanation relies on a structural feature of the Y-Ba-system. Thus, studies of antiferromagnetic order have shown[37] that the Y–Ba system has two interplane interactions of different strength [cf. (5.4)]. This compound can therefore be looked upon as a double-layer system. Friedel has used the XY model (see, for example, Ref. 37) to show that T_N in the n-layer system should be proportional to the number of layers.

The magnetic moment of copper in the Y–Ba system is approximately $0.5\mu_B$, just as in the La system. The similarity between the magnetic structures, the equal atomic magnetic moments of copper, and the strong effect of oxygen vacancies on the magnetic ordering temperature, suggest that these two systems belong to the same class of spin $S = 1/2$ magnets. Which particular system is involved will become clear from the discussion given below.

Soon after the discovery of the Y–Ba system, it was found that the replacement of Y with rare-earth elements, having high atomic magnetic moments does not affect the crystal structure, the temperature of the superconducting transition, or other superconducting properties.[38,39] This paradoxical phenomenon can be explained by recalling that

TABLE I. Magnetic ordering temperatures of copper as functions of δ in $NdBa_2Cu_3O_{7-\delta}$.

δ	T_{N1}, K	T_{N2}, K
0.9	430	80
0.8	400	40
0.65	230	10

the electron states of the rare-earth ions in the crystal lie deep under the Fermi surface. The latter is formed by electrons in CuO_2 planes, and this leads to weak exchange coupling between these states and the rare-earth ions.

A particularly detailed neutron-diffraction study of the magnetic structure of $REBa_2Cu_3O_{7-\delta}$ has been carried out with Nd as the rare-earth element.[39] A magnetic phase transition to an antiferromagnetic structure such as that shown in Fig. 14a was found, with ordering of only the copper atoms in CuO_2 layers at high temperatures and oxygen vacancy concentrations $\delta > 0.5$. The temperature T_{N1} was found to fall with increasing δ. Since the magnetic cell doubles up in the a, b but retains its dimension in the c direction, the magnetic Bragg reflections are characterized by the indices $(1/2, 1/2, l)$, where l is an integer. The temperature behavior of these materials is very typical: the intensity increases with decreasing T below T_{N1}, but does so nonmonotonically, reaching a maximum at T_{N2} and vanishing as $T \to 0$. At the same time, the $(1/2, 1/2, l/2)$ lattice reflections appear for $T < T_{N1}$, indicating the onset of a new magnetic order that corresponds to the doubling of the magnetic cell in the c direction, as well. This order corresponds to the magnetic ordering of copper ions in chains. Analysis of the neutron diffraction patterns yields the structure of Fig. 14b. The magnetic ordering of the copper atoms in chains is particularly sensitive to the parameter δ (Table I). For the compound with $\delta = 0.9$, the magnetic moment at low temperature is $(0.97 \pm 0.05)\,\mu_B$ per copper atom in the CuO_2 planes and $(0.46 \pm 0.06)\,\mu_B$ per copper atom in chains. This very considerable difference between the magnetic moments seems to us to be evidence for a noncollinear magnetic ordering of atoms in chains, so that the figure of $0.46\mu_B$ represents only the projection of the atomic magnetic moment onto the a, b plane. We note here that, according to Ref. 37, the magnetic moments of atoms in chains have not been found in the Y–Ba system, and the magnetic moments in planes were found to be $0.64\mu_B$. This question of the magnetic ordering of copper atoms in chains requires further analysis.

The magnetic ordering of the rare earth atoms occurs at very low temperatures. In the case of $ErBa_2Cu_3O_7$, the magnetic transition occurs at $T_{N3} \approx 0.5$ K. The magnetic moments of Er form the antiferromagnetic structure with unit

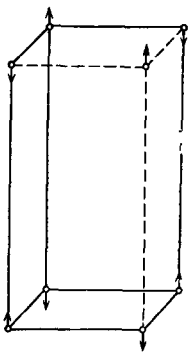

FIG. 15. Magnetic structure of the rare earth sublattice of $ReBa_2Cu_3O_{7-\delta}$.

cell twice the size in all three directions, and the magnetic moments pointing along the c axis (Fig. 15). Similar ordering is observed in compounds with other rare earth elements (Table II). The ordering temperatures of the rare earth sublattices are found to be very low because of the very weak coupling between the localized magnetic moments of the $4f$-shells and electrons on the Fermi surface, which explains the other important feature of these compounds, namely, the fact that T_c is independent of the concentration of the rare earth elements. The only exception is the compound containing praseodymium. It is already clear from Table II that Pr is different from the other rare earth elements.[40] T_{N3} for this element is higher by an order of magnitude, and the atomic magnetic moment is substantially lower for the other rare earth elements. The data of Table II are given for the nonsuperconducting compound $PrBa_2Cu_3O_7$. The other compounds, apart from Ce and, possibly, Tb and Lu, are superconductors with the high values $T_c \sim 80$–90 K in this concentration range of oxygen. Superconductivity also vanishes in the mixed compound $Y_{1-x}Pr_xBa_2Cu_3O_7$ for $x \gtrsim 0.6$ because of suppression by the paramagnetic impurity. The reason for this anomalous behavior of the Pr-containing compound is the strong hybridization of the $4f$-electrons with electron states on CuO_2 planes on the Fermi surface. This is also indicated by the anomalously high value of the parameter γ in the electronic specific heat ($\gamma \approx 196$ mJ/mole.K^2), which is comparable with values obtained for many heave-fermion systems.

The magnetic ordering observed in neutron diffraction experiments is fully correlated with thermodynamic data, e.g., with the temperature dependence of magnetic susceptibility $\chi(T)$ of La_2CuO_4, which shows a peak in the neighborhood of the Néel point.[41] The compound La_2CuO_4 is isomorphic with substances such as K_2NiF_4 and K_2MnF_4, which are well known as quasi-two-dimensional antiferromagnets. It follows from this that La_2CuO_4 should also be a quasi-

TABLE II. Magnetic ordering temperatures and atomic magnetic moments of the rare earth sublattice in $REBa_2Cu_3O_{7-\delta}$.

RE	Yb	Nd	Er	Dy	Gd	Pr
T_{N3}, K	0.35	0.5	0.5	1.0	2.2	17
μ, μ_B			4.9	7.2	7.4	0.24

two-dimensional antiferromagnet with strong predominance of exchange within planes (CuO_2) as compared with exchange between planes. The following spin Hamiltonian was proposed in Ref. 41 for the analysis of magnetic experimental data on La_2CuO_4:

$$\mathcal{H} = \sum_{\langle nn \rangle} \mathbf{S}_i \overleftrightarrow{J}_{nn} \mathbf{S}_{i+\delta}, \tag{5.2}$$

where $\mathbf{S}_i$ is the $S = 1/2$ spin operator and

$$\overleftrightarrow{J}_{nn} = \begin{pmatrix} J^{aa} & 0 & 0 \\ 0 & J^{bb} & J^{bc} \\ 0 & -J^{bc} & J^{cc} \end{pmatrix}, \tag{5.3}$$

in which the sum is evaluated over nearest-neighbor sites. This Hamiltonian includes the antisymmetric exchange (cf. the Dzyaloshinski-Moriya interaction) that describes canting of copper spins relative to the CuO_2 planes mentioned above. The corresponding parameters of the Hamiltonian are determined from experimental data[27,41] and have the following values:

$$J_{nn} \equiv \frac{1}{3}(J^{aa} + J^{bb} + J^{cc}) \approx 1200\,\text{K}, \quad J^{bc} \approx 6\text{K}.$$

For the spin interactions between the CuO_2 planes we have

$$J^{\perp} \approx 0{,}02\ \text{K}.$$

In the case of the Y–Ba system, the results reported in Ref. 3 show that the exchange interaction $J_{\parallel}$ between spins in the CuO_2 plane has the same value in the La system, but the situation is more complicated for the interaction between different planes. The CuO_2 planes form bilayers consisting of two Cu2 (02, 03) planes separated by a layer of Y atoms. The interaction between these bilayers is conveyed by Cu1—O_x chains. We shall use $J_{\perp 1}$ to denote the exchange spin interaction between planes in a bilayer, and $J_{\perp 2}$ will represent the interaction between spins in neighboring bilayers. The spin Hamiltonian for this compound can be written in the form

$$\mathcal{H} = \frac{1}{2} J_{\parallel} \sum_{i,k,\mathbf{a}} \mathbf{S}_{ik}\mathbf{S}_{i+\mathbf{a},k} + J_{\perp 1} \sum_i \mathbf{S}_{iA}\mathbf{S}_{i+\mathbf{c}_i} + J_{\perp 2} \sum_i \mathbf{S}_{iA}\mathbf{S}_{iC}, \tag{5.4}$$

where $\mathbf{a}$ is the nearest-neighbor vector on a CuO_2 plane, $\mathbf{c}$ is the nearest-neighbor vector along the $\mathbf{c}$ axis, and $k = A, C$ (cf. Fig. 14). Comparison with experimental data yields

$$J_{\parallel} \sim 1000\ \text{K}, \quad J_{\perp 1} \sim 20\ \text{K}, \quad J_{\perp 2} \sim 0.2\ \text{K}.$$

Strictly speaking, the Hamiltonian (5.4) must include the anisotropic exchange energy if we are to account for the experimental results. The magnetic properties of both the La and Y–Ba systems can therefore be regarded as those of a quasi-two-dimensional antiferromagnet. Serious evidence in favor of this conclusion is provided by studies of spin correlations in inelastic neutron scattering, which will be discussed in the next section.

The behavior of the La system in a magnetic field was examined in Ref. 31, and a new phase boundary was found on the magnetic field/temperature plane. When the magnetic field was parallel to the c axis ($\mathbf{H} \| c$), and the temperature was greater than that corresponding to the critical field $H_c(E)$, a weak induced ferromagnetic moment was observed along the c axis with $\mu_c \approx 2 \cdot 10^{-3} \mu_B$. This can be understood by recalling the crystal structure of the orthorhombic phase of La_2CuO_4 that allows weak ferromagnetism corresponding to antisymmetric exchange in the Hamiltonian (5.2)–(5.3). In the ground state, the slight canting of the antiferromagnetic moments of copper ions on the a, b plane in each CuO_2 layer produces weak ferromagnetic moments along the c axis in each layer. These moments are in antiphase between neighboring layers, and can be given ferromagnetic order by an external magnetic field. This ordering arises as a result of the 180° rotation of the antiferromagnetic moments on the a, b planes in those layers in which the weak ferromagnetic moment along the c axis points against the field. This phase transition was investigated in Ref. 31 in the mean-field approximation, and good agreement was established with experimental data on susceptibility and $H_c(T)$. The magnetic phase diagram was also examined in Ref. 31. An interesting feature of this phase transition is the considerable reduction (by a factor of roughly 2) in the resistance of the sample in the a, b plane in the ferromagnetic phase in the external field.

Antiferromagnetic ordering on the CuO_2 planes that is analogous to the ordering in La and Y–Ba systems is observed by the μSR method in the dielectric phases of $Bi_2Sr_2YCuO_x$ and by the polarized neutron method in $TlBa_2YCu_2O_7$.[51]

Interesting magnetic properties are exhibited by the new compounds $Nd_{2-x}Ce_xCuO_4$ for which electron-type conductivity is expected (see Ref. 106). For the $T < T_N = 255$ K compound Nd_2CuO_4, exhibits antiferromagnetic order of the same type as La_2CuO_4. However, additional magnetic transitions at 80 and 30 K have been observed in the former. It is assumed that the interaction between the magnetic moments of Nd^{3+} and the spins of Cu^{2+} becomes important for $T < 30$ K. Inelastic neutron scattering shows the presence of strong two-dimensional spin correlations, just as in the case of $\gamma \approx 196$.

Finally, we note Ref. 42 which reports a symmetry analysis of the kinetic structure of $YBa_2Cu_3O_{7-\delta}$ and discusses possible determinations of the parameters of the magnetic Hamiltonian from antiferromagnetic resonance and the inelastic light scattering data. Experimental data of this type would enable us to improve the values of the parameters of the Hamiltonian (5.4).

6. *Spin correlations.* The double differential cross section for the magnetic scattering of neutrons by a crystal with the transfer of energy ω and momentum $\mathbf{Q} \equiv \mathbf{k} - \mathbf{k}'$ ($\mathbf{k}$ and $\mathbf{k}'$ are the wave vectors of the incident and scattered neutron beams) can be written in the form of the Fourier transform of the pair correlation function for the spins:

$$S^{\alpha\alpha}(\mathbf{Q}, \omega) \equiv \frac{1}{2\pi} \int_{-\infty}^{\infty} e^{-i\omega t} \langle S^{\alpha}(-\mathbf{Q}, 0)\, S^{\alpha}(\mathbf{Q}, t) \rangle \, \mathrm{d}t. \tag{6.1}$$

The integral of this quantity with respect to energy determines the instantaneous correlation function

$$S^{\alpha\alpha}(\mathbf{Q}) \equiv \int S^{\alpha\alpha}(\mathbf{Q}, \omega)\, \mathrm{d}\omega = \langle S^{\alpha}(-\mathbf{Q}, 0)\, S^{\alpha}(\mathbf{Q}, 0) \rangle. \tag{6.2}$$

The quantities $S^{\alpha\alpha}(\mathbf{Q},\omega)$ and $S^{\alpha\alpha}(\mathbf{Q})$ can be measured directly with three-crystal and two-crystal spectrometers.

This type of investigation was carried out as soon as a large enough single crystal of La_2CuO_4 became avail-

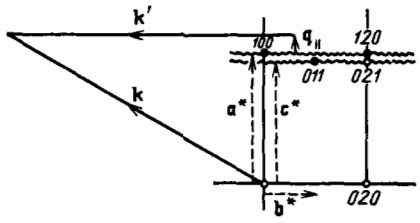

FIG. 16. Geometry of the neutron scattering experiment using La_2CuO_4 (Refs. 43 and 44). **a***, **b***, **c*** are the reciprocal lattice vectors. Wavy line shows the diffuse scattering rod.

able.[43,44] If we assume quasi-two-dimensional spin correlation in this material, we must expect that diffuse scattering in the back hemisphere, described by the quantity $S^{\alpha\alpha}(\mathbf{Q})$, will take the form of rods joining the reciprocal lattice sites in the direction perpendicular to the *a*, *c* planes, i.e., the CuO_2 planes (Fig. 16). In this experiment, the energy of the incident neutron beam was 30 meV and the (1, 0.4, 0) position on the rod corresponded to $\omega = 0$, showing that the wave vector of the scattered neutrons was always parallel to the vector **b***. This means that, in the experiment with the two-crystal spectrometer, in which for each fixed direction a measurement is made of the energy integral (i.e., the quantity $S^{\alpha\alpha}(\mathbf{Q})$, we directly obtain the two-dimensional correlation function $\langle S^{\alpha}(-\mathbf{q}_\parallel,0)S^{\alpha}(\mathbf{q}_\parallel,0)\rangle$, since the vector $\mathbf{q}_\parallel$ lies in the CuO_2 plane.

The diffuse magnetic scattering distribution by spin fluctuations is present well beyond the limits of the Néel

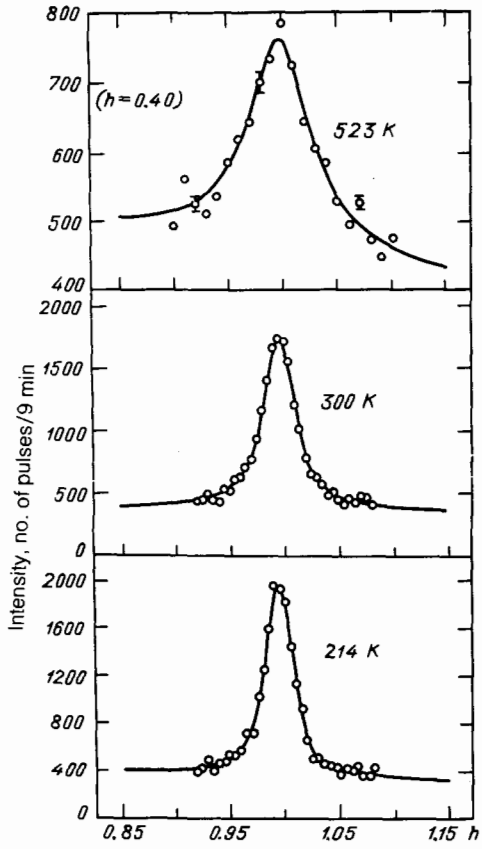

FIG. 17. Scanning of the diffuse rod in reciprocal space in the direction of the **a*** vector in the two-crystal diffractometer with the La_2CuO_4 specimen at $T = 195$ K (Ref. 45).

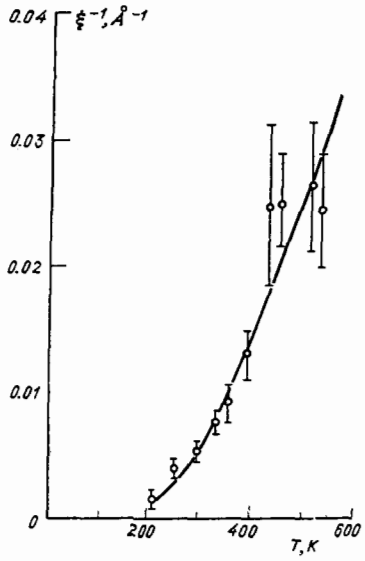

FIG. 18. Temperature dependence of the reciprocal correlation length in La_2CuO_4 (Ref. 45).

temperature. These data can be used to calculate the correlation length for instantaneous spin correlations. The results are shown in Fig. 18. The correlation length varies from 40 Å at 500 K to 400 Å at T_N.

The integral diffuse-scattering intensity rises slightly as the temperature is reduced on the way to T_N, but below the magnetic ordering temperature it begins gradually to increase, tending to zero as $T \to 0$ (Refs. 43 and 44). At the same time, the intensity of the (100) magnetic Bragg peak grows in the usual way, reaching its maximum at $T = 0$. We thus see the transformation of diffuse scattering into the Bragg peak, which is observed in two-dimensional antiferromagnets, for example, K_2NiF_4. However, this transformation is smooth in La_2CuO_4, whereas it is relatively rapid in K_2NiF_4: everything happens within the small temperature interval of about 2% of T_N. This reflects the fundamental difference between three-dimensional magnetic ordering and these planar antiferromagnets. In K_2NiF_4, i.e., an Ising type magnet, the transition to long-range order is essentially two-dimensional in character. In La_2CuO_4, on the other hand, long-range order is formed as a result of the interaction between the planes.[27] In isomorphic magnets such as La_2NiO_4 and La_2CoO_4, which have atomic spins $S = 1$ and $S = 3/2$, respectively, the phase transition to long range order is analogous to the transition in K_2NiF_4. Only La_2CuO_4, with $S = 1/2$, exhibits unique properties: in the presence of well-defined quasi-two-dimensional fluctuations, it behaves during the phase transition as a Heisenberg antiferromagnet with $S = 1/2$.

The three-crystal spectrometer has been used to investigate the dynamics of spin fluctuations. In contrast to the low-energy dynamics of spin fluctuations near the phase transition in the usual three-dimensional magnets, we now have high-energy spin excitations in La_2CuO_4 for $T > T_N$. Their dispersion is quasi-two-dimensional in character: $\omega(\mathbf{q}) = vq_\parallel$, i.e., it does not depend on the wave vector component perpendicular to the CuO_2 plane. The velocity of the spin excitations is found to be exceedingly high. For example, for $T = 300$ K, we have $v \geqslant 0.6$ eV Å. This figure agrees

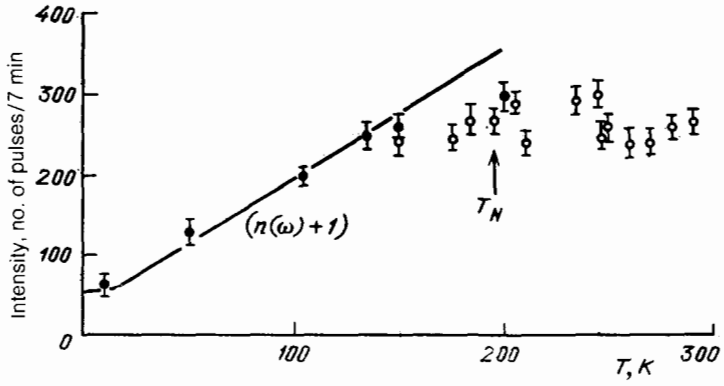

FIG. 19. Intensity of the inelastic peak with transition energy of 3 meV as a function of temperature for La_2CuO_4 (Ref. 45).

with the data obtained for spin-wave excitations, deduced from estimates of the planar exchange integral J (Ref. 40), and also data on two-magnon Raman scattering.[46]

Figure 19 shows the density of spin excitations as a function of temperature. The inelastic peak intensity is independent of T between 300 and 200 K (in the paramagnetic phase), and then falls between 5 K and 150 K, following the factor $n(\omega)+1$ with the Bose distribution function $n(\omega)$. The spin excitations of the system for $T<T_N$ are therefore the usual spin waves in the Néel state of the antiferromagnet.

We see that the $S=1/2$ Heisenberg antiferromagnet La_2CuO_4 exhibits unusual properties in the paramagnetic temperature range and in the neighborhood of T_N. They include two-dimensional spin correlations over distances of the order of 200 Å, and a relatively high energy of spin excitations. This state is called the quantum spin fluid (QSF).[43] The word "fluid" reflects the fact that the structure factor [the quantity $S^{\alpha\alpha}(\mathbf{Q})$] has a purely dynamic character.

Quantum effects play a very important part of this context. One of them consists of a significant reduction in the correlation length as compared with the classical two-dimensional Heisenberg magnet. The correlation length for the latter (in units of the lattice constant a) is given by[47]

$$\frac{\xi}{a}=\exp\frac{2\pi JS^2}{kT}. \tag{6.3}$$

If we take for La_2CuO_4 the value $JS^2=650$ K, then for $T=300$ K we obtain $\xi/a\approx 8\cdot 10^5$, which is greater by four orders of magnitude than the experimental result $\xi/a\approx 50$.[44] Next, in contrast to classical three-dimensional and two-dimensional systems, in which the slowing down of fluctuations is observed as soon as the correlation length becomes very large, it is found that La_2CuO_4 shows nothing of the kind, and the fluctuations remain of the high energy type: the velocity of spin excitations is greater by an order of magnitude than the velocity of sound in this medium. A more detailed account of the theory of two-dimensional quantum antiferromagnets is discussed in Sec. 8.

We now turn to the doped compounds $La_{2-x}M_xCuO_4$. It is clear from Fig. 2 that Sr-containing compounds exhibit the metal-insulator transition for $x\sim 0.05$. Typical hopping conductivity, described by $\ln\sigma\sim -(T_0/T)^{1/4}$, is observed for $x\lesssim 0.05$ and $T\lesssim 100$ K, and the carriers are found to be localized because of disorder. The carriers (holes) become delocalized for $x>0.05$, and the material becomes a metal and a superconductor. As we have seen, T_N depends on the concentration x of the divalent metal impurity. In the absence of long range magnetic order, doped compounds in the metallic phase can also be in the QSF state, and the high-energy spin fluctuations can be the conveyors of the pairing interaction between the electrons. This idea has stimulated detailed studies of spin fluctuations in doped systems.

Experiments with the two-crystal spectrometer have shown that the correlation length of spin fluctuations falls with increasing dopant concentration (Fig. 20). The solid line in this figure represents the function $3.8x^{-1/2}$ Å that gives the mean separation between O^- holes on the CuO_2 planes, which are introduced by the Sr impurity. It is remarkable that ξ is in very good agreement with this quantity, which suggests that the holes have a very strong destructive effect on the magnetic state of the system of Cu^{2+} ions. This effect can be partially understood in terms of the above idea of frustration of exchange coupling, although this mechanism was proposed for the description of the dielectric phase. The reduction in the correlation length with x should be correlated with the variation T_N in the magnetically ordered phase. Actually, the authors of Ref. 45 have considered the following estimated temperature of the three-dimensional phase transition in the quasi-two-dimensional model, expressed in terms of the correlation length ξ_2 of two-dimensional spin fluctuations (in units of the separation between nearest neighbors):

$$kT_N\approx J_\perp\xi_2^2(T_N). \tag{6.4}$$

The measured peak intensities, integrated with respect to the transferred energy, taking into account the entire contribution due to spin fluctuations have shown[27] that these intensities, which determine the local magnetic moment of Cu^{2+} do not depend on the impurity concentration. This leads to the following important general conclusion. Holes

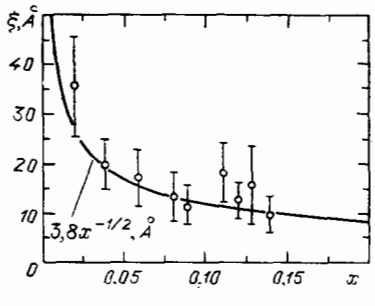

FIG. 20. Magnetic correlation length as a function of Sr concentration in $La_{2-x}Sr_xCuO_4$ (Ref. 27).

influence only the correlation between the spins of the copper ions, but have no effect on the magnitude of the atomic magnetic moment of copper in doped compounds.

Spin fluctuations in highly-doped samples are mostly high-energy fluctuations at room temperature, but even at 350 K there is a substantial fraction with energies $E<0.5$ meV, and these low energy fluctuations are three-dimensional. As the temperature T is reduced, the fraction of low-energy components is found to rise, and new Sr experiments with $La_{2-x}Sr_xCuO_4$ have shown[107] that, for $x=0$, 0.01, 0.02, and 0.05, all these spins are frozen at temperatures below about 4 K. It follows that $La_{2-x}Sr_xCuO_4$ is superconducting in the presence of the slowly fluctuating spin fluid.

Spin fluctuations in the Y–Ba system were investigated in Ref. 37. At $T=200$ K, the antiferromagnet $YBa_2CuO_{6.3}$ with $T_N\approx 350$ K, was found to produce peaks corresponding to inelastic magnetic scattering in the $(q, q, 0)$ direction for transferred energies of 3 and 6 meV, and the intensity decreased as a function of the transferred energy. The width of these peaks increased from 0.07 $Å^{-1}$ at 3 meV to 0.1 $Å^{-1}$ at 6 meV. This behavior of the peak widths, and also the observed asymmetry of the peak at 3 meV, was explained by the spin-wave contribution. Since the resolution of the spectrometer was not good enough to produce two well-resolved peaks, the experiment revealed an asymmetric peak. A similar result was obtained in Ref. 27 for La_2CuO_4. Estimates of the spin-wave velocity gave ~ 0.4 eV Å.

A more detailed investigation of spin waves in a single-crystal of $YBa_2Cu_3O_{6.3}$ was undertaken in Ref. 48b. Comparison of the experimental data with the theory based on the Hamiltonian (5.4) was used to determine the parameters of the latter. The resulting values have already been listed above. In addition, an estimate was made of the anisotropic exchange energy, and the result was ~ 0.0035 meV. For transferred energies of 3, 9, and 15 meV and $T=300$ K, inelastic-scattering peaks were observed but could not be resolved for the two values $\mathbf{q}_\parallel$ and $-\mathbf{q}_\parallel$ because of the strong dispersion of the excitations. These experiments demonstrated that the lower limit of the spin-wave velocity was 0.5 eV Å, which is in good agreement with the results deduced from inelastic light-scattering data.[49] Dispersion along the c axis was found to be slight. The temperature dependence of the inelastic scattering intensity showed that spin correlations in the CuO_2 planes persisted up to temperatures of at least 100 K above T_N. Although rather limited, these data may be regarded as confirmation of the quasi-two-dimensional character of magnetism in $YBa_2Cu_3O_{7-\delta}$ for $\delta\gtrsim 0.5$.

Further confirmation of this can be seen in magnetic susceptibility data.[29] For samples with a low oxygen content ($\delta\approx 1$) the susceptibility $\chi(T)$, has a maximum for high temperatures T, and falls smoothly with decreasing temperature. This behavior is typical for spin correlations in two-dimensional antiferromagnets. The susceptibility $\chi(T)$ varies very slowly with increasing oxygen content, approaching the temperature-independent form for $\delta\approx 0$. This gradual variation shows that the antiferromagnetic correlations survive in orthorhombic phase, just as they do in $La_{2-x}M_xCuO_4$.

Until now, there has been very little information on magnetism in the superconducting phase of the Y–Ba systems. Polarized-neutron scattering by powders has indicated the existence of low-energy spin fluctuations in $YBa_2Cu_3O_{6.6}$ (Ref. 50). The μSR method[36] has revealed that, although the long-range antiferromagnetic moment decreases with decreasing δ, the local magnetic moment remains constant, at least in the tetragonal phase. Attempts to detect inelastic magnetic scattering at energies below 20 meV in the superconducting phase of $YBa_2Cu_3O_{7-\delta}$ (Ref. 48b) have been unsuccessful.

Summarizing the experimental studies of known classes HTSCs, we conclude that the onset of long range magnetic order, or magnetic fluctuations, in the copper sublattice is closely related to the onset of the superconducting state and to its properties in both $La_{2-x}Sr_xCuO_4$ and $YBa_2Cu_3O_{7-\delta}$, and superconductivity appears for high enough x or large $\delta\approx 1$, and superconductivity appears for high enough x or small δ (this is the anticorrelation between magnetic and superconducting order parameters), there are ranges of x and δ in which the two phenomena co-exist or at least interfere. Since the mechanism responsible for superconducting pairing in these HTSCs has not as yet been discovered, it is tempting to perform a theoretical investigation of pairing via spin excitations of the particular magnetic state found in these materials, which is referred to as the quantum spin fluid (QSF). This is more likely to be the superproblem for the theory. The current problem is the theoretical analysis of the QSF state and the interpretation of the change in the magnetic state of these systems as a result of doping.

II. ATTEMPTED THEORETICAL INTERPRETATIONS

7. *Magnetism and superconductivity in quasi-two-dimensional systems with strong electron correlation.* Extensive experimental data are now available on the magnetic and superconducting properties of high-temperature superconducting compounds. Their most obvious property is the high sensitivity to changes in the number of electron holes produced on doping, but they also exhibit the metal-insulator phase transition. Both phenomena have long been known in other materials, and different theoretical models have been proposed for their interpretation. An important place among them is occupied by the Hubbard model that allows for strong electron correlations in a narrow band. The Hubbard Hamiltonian is

$$\mathcal{H}=-t\sum_{\langle ij\rangle\sigma}c_{i\sigma}^{+}c_{j\sigma}+U\sum_i n_{i\uparrow}n_{i\downarrow}, \tag{7.1}$$

where the first term describes the transfer of electrons with spin σ from site i to the nearest site j, whereas the second term represents the repulsion energy between two electrons with opposite spins on site i. In the case of a narrow band, the Coulomb repulsion is large ($U\gg t$), and the model provides a description of the metal-insulator phase transition (Mott transition) as well as many physical properties that depend on the band population (see, for example, Refs. 17 and 52). Since it is likely that $U\gtrsim t$ in copper oxide HTSCs, immediate and numerous attempts were made to use the Hubbard model in the description of HTSCs. In view of the importance of the electron states of CuO_2 layers, and the quasi-two-dimensional character of the electron spectrum, we have to devote particular attention to the properties of the two-dimensional Hubbard model.

The statistical mechanics of the Hubbard model is a very complicated subject that has not been adequately investigated. Attempts to understand the physics of the two-dimensional case can be made from two points of view: either by using the results of the three-dimensional model, which has been extensively investigated, or by considering the one-dimensional problem for which there is an exact solution.[53]

From among the numerous results obtained with the three-dimensional Hubbard model, we mention those that may be of interest for our discussion here. For a half-filled band, for which the number of electrons N_e is equal to the number of atoms N_a, i.e., $N_e/N_a \equiv n = 1$, the Hubbard model has an antiferromagnetic ground state.[52] As we depart from the half-filled state ($n \neq 1$), the behavior of the system is described by the exact result obtained by Nagaoka[54] and stating that, as $U \to \infty$, the ground state is a ferromagnet for $N_e = N_a \pm 1$. (We note, by the way, that Anderson[68] has recently thrown some doubt on the validity of the Nagaoka theorem,[54] at least in the two-dimensional case.)

The physical justification for the above result relies on the fact that excess carriers can move freely through neighboring atoms if their spins are parallel to the spins of the atoms, and this results in a reduction in their kinetic energy. Ferromagnetism is possible for finite values of U, even if the concentration of excess carriers is finite (Fig.21).

A remarkable consequence of the exact solution of the one-dimensional Hubbard model is that it is in principle impossible to reduce it to the Fermi-fluid type Landau picture in which the introduction of the interaction between electrons in the electron gas does not affect the Fermi momentum and influences only the size of the jump Z in the particle momentum distribution at the Fermi momentum. This conclusion has far-reaching consequences and is beautifully illustrated by the graph of n as a function of $\mathbf{Q}$ which, in the exact one-dimensional solution of Lieb and Wu, plays the part of the Fermi momentum[55] (Fig. 22).

It is readily seen that, for $n = 1$, the quantity $\mathbf{Q}$ is numerically equal to $\pi/2$ for noninteracting electrons and to π for interacting electrons. This is so because, in the one-dimensional Hubbard model, any weak interaction ($U \neq 0$) leads to a dielectric ground state.[53] Its Hamiltonian can be reduced to the Hamiltonian for the Heisenberg model of an antiferromagnet.[56] The ground state of the one-dimensional Heisenberg antiferromagnet has a long history that began with the invention of the Bethe ansatz (see, for example, Ref. 57), which can be used to obtain the exact solution for the ferromagnetic or antiferromagnetic chain of $S = 1/2$ spins.

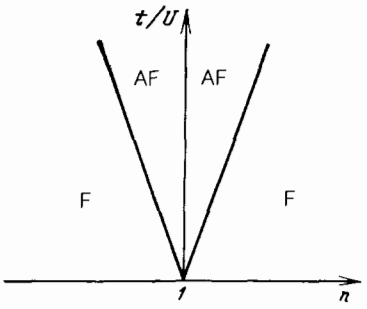

FIG. 21. Phase diagram of magnetic states in the three-dimensional Hubbard model ont he $t/U,n$ plane.

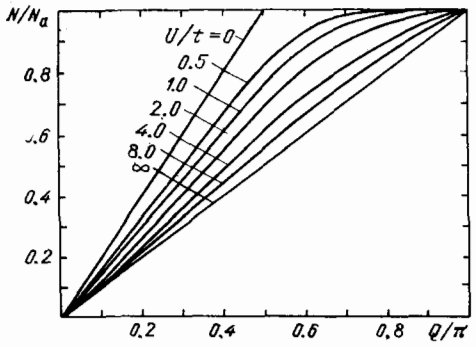

FIG. 22. n as a function of Q for different values of U/t (Ref. 55).

The ground state of the antiferromagnetic chain is a singlet, and analysis of the spectrum of elementary excitations performed by Takhtajan and Faddeev[58] has shown that a "spin wave" on an antiferromagnetic chain can be represented by two neutral fermions (kinks) of spin 1/2. In other words, neutral fermions are the elementary excitations of the one-dimensional antiferromagnetic Heisenberg chain.

Anderson[59] has proposed that the two-dimensional antiferromagnet should exhibit some of the properties of one-dimensional systems. In particular, for the completely frustrated triangular lattice of half spins, the ground state can be constructed by analogy with the exact singlet Bethe ground state of the linear antiferromagnetic chain.

Each pair of neighboring spins on a plane lattice is assumed to be in the singlet state relative to one another, and there is a constant variation in the combination of neighboring spins into pairs. In other words, the "bonds" between nearest neighbors can travel or resonate by analogy with the way "double" and "single" (valence) bonds resonate in the benzene ring. This state of the spin system is a superposition of all the realizations of singlet pairs, and is described by analogy with quantum chemistry as a state with resonating valence bonds (RVB).

Consider a planar square lattice. It belongs to a class of lattices that can be imagined as two interpenetrating lattices, and can therefore be said to have "black and white symmetry", i.e., there are two types of site (black and white) and, generally, four types of bond ending on four sites, e.g., white, surrounding a black site. The RVB state can then be looked upon as a superposition of all the "instantaneous" pictures of the form shown in Fig. 23. It has a lower energy than the Néel state with long-range antiferromagnetic order if the interactions after the nearest-neighbor interactions are antiferromagnetic and strong enough, so that, just as in the triangular lattice, we again have frustration.

Since the Hubbard-Hamiltonian near the half-filled band with $U \gg t$ is actually identical with the Hamiltonian for the Heisenberg antiferromagnet, Anderson suggested

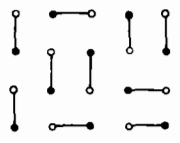

FIG. 23. One of the components forming the "vacuum" state in a system with resonating valence bonds.[62] The lines represent the valence bonds.

that the ground state of the two-dimensional Hubbard model should be a RVB state.[60]

Let us now present the basic assumptions and conclusions of RVB theory. If $n \approx 1$, $U \gg t$, it is convenient to replace the Hamiltonian (7.1) with the effective Hamiltonian in which virtual states with doubly populated sites have been excluded by a canonical transformation, so that only singly populated sites remain:[61]

$$\mathcal{H} = -t \sum_{\langle ij\rangle,\sigma} (1-n_{i,-\sigma})\, c_{i\sigma}^{+} c_{j\sigma} (1-n_{j,-\sigma}) - \mu \sum_{i\sigma} n_{i\sigma} + J \sum_{\langle ij\rangle} \left(\mathbf{S}_i \mathbf{S}_j - \frac{1}{4} n_i n_j\right), \tag{7.2}$$

where

$$S_i^{+} = c_{i\uparrow}^{+} c_{i\downarrow}, \quad S_i^{-} = c_{i\downarrow}^{+} c_{i\uparrow}, \quad S^z = \frac{1}{2}(n_{i\uparrow} - n_{i\downarrow}); \tag{7.3}$$

$n_i = n_{i\uparrow} + n_{i\downarrow}$, μ *is the chemical potential, and* $J = 4t^2/U$ *is* the exchange parameter of the effective antiferromagnetic interaction.

We now introduce the creation operator for the singlet valence-coupled pair on sites i and j:

$$b_{ij}^{+} = \frac{1}{\sqrt{2}} (c_{i\uparrow}^{+} c_{j\downarrow}^{+} - c_{i\downarrow}^{+} c_{j\uparrow}^{+}), \tag{7.4}$$

so that, in terms of the effective Hamiltonian, (7.2) can be written as the sum of two terms describing, respectively, the kinetic energy of electrons in the almost filled bottom Hubbard band and the interaction energy of the singlet pairs:

$$\mathcal{H}_{\text{eff}} = -t \sum_{\langle ij\rangle,\sigma} (1-n_{i,-\sigma})\, \bar{c}_{i\sigma}^{+} c_{j\sigma} (1-n_{j,-\sigma}) - \mu \sum_{i,\sigma} n_{i\sigma} - J \sum_{\langle ij\rangle} b_{ij}^{+} b_{ij}. \tag{7.5}$$

Before we turn to a systematic investigation of the states determined by this Hamiltonian, we must provide, following Kivelson,[63] a qualitative picture of the excited states that appear above the vacuum (Fig. 23) in which all the corners are occupied by electrons (one per site) that form singlet pairs with their neighbors. Neutral fermions (spinons) and charged bosons (holons) are of this kind.

To understand the origin of these excitations, we must remember that each lattice site with $n_i = 1$ is neutral, but not spinless. In the ground state, each site participates in one valence bond, so that two unpaired electrons are produced when one valence bond is broken (Fig. 24). If we compare this with the vacuum state, we can describe it in terms of the appearance of two quasiparticles localized on lattice sites with spin half and zero charge. We thus arrive at the concept of a neutral fermion, i.e., the spinon.

Another type of vacuum excitation appears if an electron is removed from a given site (by excitation to another band or by doping). The resulting hole has the charge e^{+},

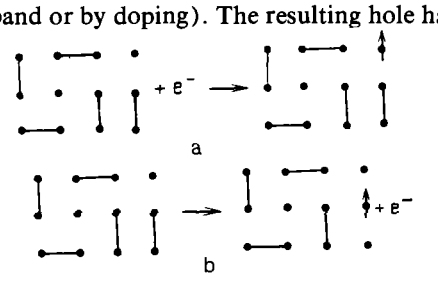

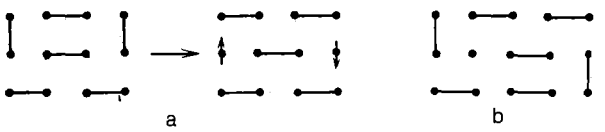

FIG. 24. Excited states in the RVB system:[63] a—two spins due to the breaking of one valence pair with spinons indicated by the arrow, b—one holon for a less than half-filled band.

but the excited state must be assigned zero spin. The result is a charged Bose quasiparticle, called the holon (cf. Fig. 24b). The charge and spin have to be separated from one another to produce excited states of a system with RVB. Figure 25 illustrates the interaction of a real electron with quasiparticle excitations of the RVB system, i.e., spinons and holons.

Having introduced the very pictorial concepts of quasiparticles in a system with RVB, we now proceed to the description of the system based on the Hamiltonian (7.5). The first attempt to employ this very complicated Hamiltonian was made by the self-consistent field method.[64] A closely related problem is the derivation of the equation for the order parameter, defined as the expectation value of the singlet pair creation operator

$$\Delta_{ij}^{*} = \langle b_{ij}^{+} \rangle. \tag{7.6}$$

In the mean-field approximation, the Hamiltonian (7.5) takes the form[64,65]

$$\mathcal{H}_{MF} = \sum_{k,\sigma} (\varepsilon_{\mathbf{k}} - \mu)\, c_{\mathbf{k}\sigma}^{+} c_{\mathbf{k}\sigma} - \sum_{\mathbf{k}} (\Delta_{\mathbf{k}} c_{\mathbf{k}\uparrow}^{+} c_{-\mathbf{k}\downarrow}^{+} + \Delta_{\mathbf{k}}^{*} c_{-\mathbf{k}\downarrow} c_{\mathbf{k}\uparrow}), \tag{7.7}$$

where

$$\Delta_{\mathbf{k}} = \sum_{\mathbf{k}'} V_{\mathbf{k}\mathbf{k}'} \langle c_{-\mathbf{k}'\downarrow} c_{\mathbf{k}'\uparrow} \rangle,$$

$$V_{\mathbf{k}\mathbf{k}'} = J[\cos(k_x - k_x') + \cos(k_y - k_y')], \tag{7.8}$$

$$\varepsilon_{\mathbf{k}} = -tx(\cos k_x + \cos k_y). \tag{7.9}$$

The quantity $x = 1 - n$ describes the deviation from the half-full population. The Hamiltonian (7.7) is formally analogous to the Hamiltonian in the Bardeen-Cooper-Schriffer (BCS) model Hamiltonian. The standard diagonalization procedure applied to the quadratic form gives the following mean-field equations for the order parameter $\Delta_{\mathbf{k}}$ and the chemical potential μ:

$$\Delta_{\mathbf{k}} = \sum_{\mathbf{k}'} V_{\mathbf{k}\mathbf{k}'} \frac{\Delta_{\mathbf{k}'}}{2E_{\mathbf{k}'}} \operatorname{th} \frac{E_{\mathbf{k}'}}{2T}, \tag{7.10}$$

$$\frac{1}{N} \sum_{\mathbf{k}} \frac{\varepsilon_{\mathbf{k}} - \mu}{E_{\mathbf{k}}} \operatorname{th} \frac{E_{\mathbf{k}}}{2T} = x; \tag{7.11}$$

where

$$E_{\mathbf{k}} = [(\varepsilon_{\mathbf{k}} - \mu)^2 + |\Delta_{\mathbf{k}}|^2]^{1/2} \tag{7.12}$$

is the quasiparticle energy.

FIG. 25. Interaction between an electron and a spinon and holon[63]: a—spinon produced from a holon when an electron is added, b—spinon and holon produced by removing an electron from the valence bond.

The authors of Ref. 64 at first assumed that the order parameter Δ_{ij} was the same for all four types of bond that end on the four nearest neighbors, i.e., $\Delta_1 = \Delta_2 = \Delta_3 = \Delta_4$. This assumption reduces to the following expression for $\Delta_{\mathbf{k}}$ as a function of the momenta:

$$\Delta_{\mathbf{k}} = \Delta_s (\cos k_x + \cos k_y), \tag{7.13}$$

which contains the same phases in the k_x and k_y directions. This form of the solution corresponds to the s-symmetry. It was subsequently found[65] that there is a solution with d-symmetry:

$$\Delta_{\mathbf{k}} = \Delta_d (\cos k_x - \cos k_y), \tag{7.14}$$

and also a solution describing the so-called mixed state:

$$\Delta_{\mathbf{k}} = \Delta (\cos k_x + i \cos k_y). \tag{7.15}$$

Analysis of (7.10) and (7.11) then showed that the solutions with s- and d-symmetry are equivalent in the half-filled case. This equivalence is a reflection of $U(1)$ gauge symmetry (invariance of the Hamiltonian under the transformation $c_{i\sigma}^+ \to e^{i\theta_i} c_{i\sigma}^+$), which can be used to transform solutions with s- and d-symmetry into one another in the half-filled case. However, this symmetry does not occur in the mixed state, which suggests that there may be a more general gauge symmetry. We shall return to this point later.

Let us now consider the expression for the quasiparticle energy (7.12). For half-filled band $x = 0, \mu = 0$, this expression reduces to $E_{\mathbf{k}} = |\Delta_{\mathbf{k}}|$. in particular, for the s-like solution,

$$E_{\mathbf{k}} = \Delta_s |\cos k_x + \cos k_y|, \tag{7.16}$$

and the spectrum becomes gapless for lines determined by the equation $\cos k_x + \cos k_y = 0$. For the mixed state, the spectrum

$$E_{\mathbf{k}} = \Delta (\cos^2 k_x + \cos^2 k_y)^{1/2} \tag{7.17}$$

becomes gapless only at the points $\mathbf{k} = (\pm \pi/2, \pm \pi/2)$. A gapless spectrum presupposes that the specific heat depends on a power of temperature [the first power for (7.16) and the second for (7.17)]. It is interesting to compare this with the well-known result for heavy fermions in the three-dimensional problem for which the gapless line spectrum gives a quadratic dependence of the specific heat on temperature, and a gapless point spectrum gives a cubic dependence.

The fundamental task in the two-dimensional Hubbard model near the half-filled state is to construct the phase diagram on the T, x plane. Anderson tried to deduce this diagram (Fig. 26) from simple physical ideas.[68] Thus, first, there is the line of phase transitions $T_0(x)$ to the RVB state (dashed line), which can be obtained in the self-consistent field approximation from the solution of (7.10) and (7.11). Second, as already noted, for the exactly half-filled band, the ground state must be an antiferromagnet and a dielectric in the three-dimensional case. It is clear, that however weak the interaction between the planes, the temperature T_N of the phase transition to the magnetically ordered state will be determined by the strength of this interaction. The $T_N(x)$ curve should fall rapidly with increasing hole concentration x because the destruction of antiferromagnetic order produces a gain in the kinetic energy of the holes. Further increase in x is accompanied by a phase transition from the dielectric to the metallic state (wavy line) in which one can expect the appearance of superconductivity. This requires further explanation. If we compare Fig. 26 with the experimental phase diagram for $La_{2-x}Sr_xCuO_4$ (Fig. 2), we find that they are similar at least at the qualitative level, if we identify the structural tetragonal-orthorhombic phase transition with the phase transition to the RVB state.

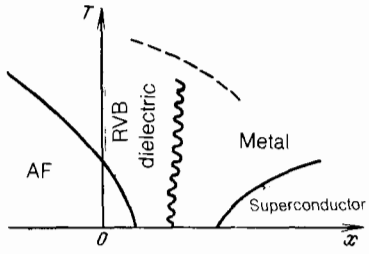

FIG. 26. Anderson's phase diagram on the T, x plane.[68]

The appearance of superconductivity in RVB theory is related to the existence of holons. Since holons are bosons, it was initially suggested[67,69] that their Bose condensation ends in a superfluid state and, hence, a superconducting state, since holons are charged particles. However, this mechanism was found to be inconsistent because, although holons are bosons, they cannot be subjected to Bose condensation as they would then have to satisfy an exclusion principle by analogy with Fermi particles. They cannot, therefore, accumulate in any particular state.[68] A superconductivity mechanism based on the pairing of holons,[68] followed by their transition from layer to layer, was subsequently proposed.[68] It would appear that a complete explanation of high-temperature superconductivity could not be found within the framework of the two-dimensional theory alone, so that the Hamiltonian describing the pure two-dimensional model had to be augmented by a term representing the hoping of electrons from one plane to another. The following picture of the onset of superconductivity state in this quasi-two-dimensional system has been proposed.[68]

In the normal state, an electron hole decays into a spinon and a holon, which is readily seen by inspection of Fig. 25. This process can be described mathematically in terms of the following representation of the electron operator:[69]

$$c_{i\sigma}^+ = e_i S_{i\sigma}^+ + \sigma d_i^+ S_{i,-\sigma}, \tag{7.18}$$

where e_i, d_i^+ are boson operators with the following meaning: e_i is the operator for the annihilation of an empty site (holon), d_i^+ is the operator for the creation of a doubly filled site (twin), and $U \to \infty$ is the operator for the creation of a neutral fermion on a site (spinon). In the limit as $U \to \infty$, the contribution of the doubly occupied sites is unimportant, so that the second term of (7.18) can be neglected and

$$c_{i\sigma}^+ \approx e_i S_{i\sigma}^+, \tag{7.19}$$

which interprets the creation of an electron as the annihilation of a hole and the creation of a spinon on the same site. It is important to note that holons and spinons are confined to a plane and cannot leave it because the separation of charge and spin degrees of freedom is performed only in a plane. On the other hand, a pair of holons is equivalent to a singlet pair

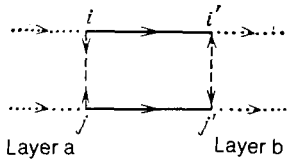

FIG. 27. Transition of a pair of holons from one plane to another.[68] Solid line—electron pair, dotted line—holon, dashed line—spinon.

of electrons, and can move from plane to plane. This process can be represented by the diagram of Fig. 27. We thus see that boson pairing can be used to find the superconducting state. The estimate of T_c given in Ref. 68 is $T_c \sim t_c^2/J$ or $T_c \sim t_c^4/J^3$, depending on the form of the boson spectrum (t_c is the integral representing the transfer of electrons between planes).

The above mechanism of superconductivity predicts high T_c of the order of the typical electron energy, but it is too complicated to be satisfactory. The idea of the RVB state, and the existence of new types of excitation, i.e., neutral fermions and charged bosons, is undoubtedly potentially useful in any search for a new mechanism of electron pairing. The problem is not only physical, but also largely mathematical because of the exceptional complexity of the model Hamiltonian (7.2) or the equivalent (7.5). Even when the kinetic term is written in the simplified form examined in Refs. 61 and 64, the mathematical difficulties are enormous.

In view of the foregoing, it is important to establish the fundamental properties of this model, including the internal symmetry of the Hamiltonian. We have already noted the U(1) gauge symmetry of the Hamiltonian (7.5) in the half-filled case. In accordance with the well-known Elitzur theory (cf. for example, Ref. 17b), this local symmetry cannot be broken, so that the mean value is $\Delta = 0$ at all temperatures, and the temperature of transition to RVB states is zero for the half-filled case. It has also been found that this system is invariant under the local SU(2) gauge transformation.[66] To demonstrate this, let us examine the Heisenberg Hamiltonian

$$\mathcal{H} = J \sum_{\langle ij \rangle} \mathbf{S}_i \mathbf{S}_j$$

in the Hubbard model for large U. We shall use the pseudofermion representation of $S = 1/2$ spin operators:

$$\mathbf{S}_i = \frac{1}{2} \sum_{\alpha\beta} c_{i\sigma}^+ \boldsymbol{\sigma}_{\alpha\beta} c_{i\beta}, \quad \sum_{\alpha} c_{i\alpha}^+ c_{i\alpha} = 1 \tag{7.20}$$

where $\boldsymbol{\sigma}$ is a vector with components taken from the Pauli matrices. The relationship given by (7.20) can readily be written in the form

$$\mathbf{S}_i = \frac{1}{4} \operatorname{Tr} \psi_i^+ \psi_i \boldsymbol{\sigma}^T, \tag{7.21}$$

where $\boldsymbol{\sigma}^T$ is the transpose of the Pauli matrix and ψ_i is a 2×2 matrix with operator components:

$$\psi_i \equiv \begin{pmatrix} c_{i+} & c_{i-} \\ c_{i-}^+ & -c_{i+}^+ \end{pmatrix}. \tag{7.22}$$

This representation can be used to rewrite the Heisenberg Hamiltonian in the form

$$\mathcal{H} = \frac{J}{16} \sum_{\langle ij \rangle} (\operatorname{Tr} \psi_i^+ \psi_i \sigma^T)(\operatorname{Tr} \psi_j^+ \psi_j \sigma^T), \tag{7.23}$$

from which it is clear that it is invariant under the gauge transformation

$$\psi_{i\alpha\beta} \to h_{i\alpha\gamma} \psi_{i\gamma\beta}, \tag{7.24}$$

where the SU(2) matrices h_i depend on the site index.

The demonstration of local SU(2) gauge symmetry leads to an order parameter formed by SU(2) matrices of the form

$$\langle \psi_i \psi_j^+ \rangle = \begin{pmatrix} -\chi_{ij}^+ & \Delta_{ij} \\ \Delta_{ij}^+ & \chi_{ij} \end{pmatrix}, \tag{7.25}$$

where

$$\Delta_{ij} = \langle c_{i+} c_{j-} - c_{i-} c_{j+} \rangle, \qquad \chi_{ij} = \sum_{\alpha} \langle c_{i\alpha}^+ c_{j\alpha} \rangle; \tag{7.26}$$

in which Δ_{ij} is the U(1) gauge field (7.6) and χ_{ij} is the U(1) gauge field previously used in Ref. 70. We thus have the possibility of describing the RVB theory by means of lattice SU (2) gauge theories.

We note at this point that the two-dimensional single-band Hubbard model has also been the subject of numerous calculations by methods whose advantage was that they were independent of uncontrollable approximations. The phase diagram (U/t,x), obtained by numerical methods, was presented by Baskaran in a review paper.[71] The RVB region was identified on this diagram with disordered magnetic moments between the ferromagnetic and antiferromagnetic regions. For $x = 0$, the ground state is antiferromagnetic. Variational Monte Carlo calculations have also been carried out. According to Ref. 72, a hole concentration of about 20% is necessary for the stabilization of the RVB state, which differs by an order of magnitude from the figure predicted by the Anderson theory.

The (t-J)-model described by the Hamiltonian (7.5) has also been investigated by the method of exact diagonalization of small two-dimensional systems. In particular, the authors of Ref. 73 examined the properties of such systems with a high hole concentration ($N_h = 4$, $N = 16$), and found that this reduced the antiferromagnetic correlation length. Moreover, there was a tendency for the holes to pair off in the intermediate regime of exchange coupling with $J/t \sim 0.4$, in contrast to the formation of hole droplets when $J/t \gtrsim 1.2$.

Approximate methods have to be used when models with a macroscopic number of particles are examined. For example, the authors of Ref. 74 used a variational method to examine the wave function proposed by Anderson for the RVB state $|\varphi\rangle = P_d |\varphi_0\rangle$, where

$$P_d = \prod_i (1 - n_{i\uparrow} n_{i\downarrow})$$

is the Gutzwiller projection operator and $|\varphi_0\rangle$ is the BCS wave functions. The authors of Ref. 74 used the Gutzwiller approximation for the projection operators, and replaced the Hamiltonian (7.5) with a renormalized Hamiltonian in which the projection operators were in turn replaced with renormalizing factors. Next, and in contrast to the superconductivity mechanism in the Anderson RVB theory (holon superfluidity), the authors of Ref. 74 assumed that the superconducting state could be characterized by the order pa-

rameter

$$\Delta_{SC} = \langle \varphi | c_{i\uparrow}^{+} c_{j\downarrow}^{+} - c_{i\downarrow}^{+} c_{j\uparrow}^{+} | \varphi \rangle, \tag{7.27}$$

which is linearly related to the parameter $\Delta_{RVB} \equiv \{\varphi_0 | c_{i\uparrow}^{+} c_{j\downarrow}^{+} - c_{i\downarrow}^{+} c_{j\uparrow}^{+} | \varphi_0\rangle$ that characterizes the RVB state [cf. (7.6) and (7.7)], where $\Delta_{SC} \sim \chi \Delta_{RVB}$. The dependence of Δ_{RVB} and Δ_{SC} on x was determined, and the significant point is that $\Delta_{SC} = 0$ and Δ_{RVB} is finite for $x = 0$. This is in agreement with the SU(2) gauge symmetry for $x = 0$.

The two-dimensional Hubbard model with a magnetic field was examined in Ref 75 for $U \gg t$. The phase diagram on the (x,h) plane was found, where h is the magnetic field. It was shown that phase transitions on this diagram were of the first order, with the exception of the case of small n and high fields for which there is a second-order phase transition to the ferromagnetic superconducting state.

The alternative to the introduction of additional fields (holons and spinons) in the investigation of the effective Hamiltonian (7.2) is the method of Hubbard operators which automatically takes into account the splitting of the electron band (at the level of the commutation relations) into the upper and lower Hubbard sub-bands for $U \gg t$. The method of Green's functions was used in Ref. 76 to derive an expression for the superconducting order parameter Δ_{ij} (7.27) which, in contrast to the mean-field approximation for holons in (7.8), contains contributions due to both the kinetic term $\sim t$ and the exchange term $\sim J$ in (7.2). However, the rigorous condition for the absence of pairing of particles in the same band on the same site leads to the d-wave symmetry of the order parameter (7.14) for which only the exchange term provides a nonzero contribution, as in the case of (7.8).

In conclusion, let us compare the properties of the above model with the physical properties of copper oxide HTSCs. The Anderson theory is confined to one nondegenerate narrow band near the half-filled state. If we compare the results of this theory with the properties of copper oxide HTSCs, we have to take into account the existence of the CuO_2 planes which must be described by the two-sublattice model[77] in which one of the sublattices is assigned to the d-states of Cu and the other to the p-states of O. If we retain only direct electron transitions between nearest neighbors, i.e., the Cu and O ions, then we can use perturbation theory to eliminate the p-sublattice and confine our attention to the d-sublattice. The effective transfer parameter t_d between neighboring ions is then given by

$$t_{\mathrm{d}} = \frac{t_{\mathrm{pd}}^2}{\varepsilon_{\mathrm{p}} - \varepsilon_{\mathrm{d}} + V}, \tag{7.28}$$

where ε_d and ε_p are the atomic levels of Cu and O, V is the Coulomb interaction between them, and t_{pd} is the transfer integral. Thus, when holes are present in the oxygen sublattice, which occurs in the HTSCs after doping, they can move inside the copper sublattice. The single-band Hubbard model can therefore be used to describe the physical properties of HTSCs (cf. Ref. 78).

We note that the validity of the last result was questioned by the authors of Ref. 108, who used the exact solution for a model of the motion of holes on CuO_2 planes with a ferromagnetic background. However, it was shown in Ref. 109 that, even in this case, the band of states splits, and becomes equivalent in all its characteristics (density of states, dispersion law, and eigenfunctions) to the single-band model with the $(t$-$J)$effective Hamiltonian.

8. *Two-dimensional Heisenberg antiferromagnet with spin 1/2.* The RVB theory of the two-dimensional Hubbard model in the limit of large U has recently given rise to considerable interest in the properties of isotropic two-dimensional Heisenberg antiferromagnets as the simplest systems for which there is some hope of finding Fermi type excitations, i.e., the analogs of neutral fermions in the Hubbard model. Attempts have been made to introduce into the two-dimensional model the ideas that arose in the exact solution of the one-dimensional Heisenberg model.

We begin by recalling some of the fundamental results found for the one-dimensional model. In 1961, Lieb *et al*[79] proved a theorem stating that an antiferromagnetic periodic chain of 1/2 spins of length L has low-energy excitations with energy of the order of $1/L$. This theorem can be trivially extended to the case of arbitrary half-integral spins, but not to the case of integral spins. We thus encounter a situation whereby systems with integral and half-integral spins exhibit different behavior.[80] In its modern version, the theorem of Ref. 79 states that, in the case of half integral spins, and in the limit of an infinite chain, the ground state is either degenerate or there are gapless excitations.[81] In the former case, the degeneracy of the ground state should be the result of spontaneous symmetry breaking. The nondegenerate state with a gap in the excitation spectrum is impossible for systems of half-integral spins and, conversely,this state can occur for systems with integral spins. The exact solution for the Heisenberg antiferromagnetic chain shows that the ground state is not degenerate and that the Descloizeaux-Pearson dispersion relation for the single-particle excitations has the form

$$E_k = \pi J |\sin k|. \tag{8.1}$$

Thus, in accordance with the theorem of Ref. 79, the excitation spectrum is indeed gapless.

The difference between systems with integral and half integral spins in one dimension is more simply investigated in the so-called nonlinear σ-model[80-83] which may be looked upon as the semiclassical limit of the Heisenberg antiferromagnet with high spin. It can be formulated as a field theory for the unit vector $\mathbf{n}(x,t)$ that describes the local variation of the direction of the Néel order parameter.

The Hamiltonian of the σ-model is derived from the standard Heisenberg Hamiltonian

$$\mathcal{H} = J \sum_i \mathbf{S}_i \mathbf{S}_{i+1} \tag{8.2}$$

by transforming to the new variables

$$\begin{aligned} \mathbf{n}_{2i} &= (\mathbf{S}_{2i} - \mathbf{S}_{2i+1}) \{2[S(S+1)]^{1/2}\}^{-1}, \\ \mathbf{l}_{2i} &= \frac{1}{2}(\mathbf{S}_{2i} + \mathbf{S}_{2i+1}). \end{aligned} \tag{8.3}$$

In the functional approximation, and in the limit of high S, we find from (8.2) that the σ-model Hamiltonian is

$$\frac{\mathcal{H}_\sigma}{2J[S(S+1)]^{1/2}} = \int \left[\frac{g}{2} \left(\mathbf{l} + \frac{\theta}{4\pi} \frac{d\mathbf{n}}{dx} \right)^2 + \frac{1}{2g} \left(\frac{d\mathbf{n}}{dx} \right)^2 \right] dx, \tag{8.4}$$

where $g = 2/[S(S+1)]^{1/2}$ is often referred to as the cou-

pling constant and $\theta = 2\pi\sqrt{S(S+1)}$ is the topological angle. The vectors $\mathbf{n}$ and $\mathbf{l}$ satisfy the relations $(\mathbf{nl}) = 0$, $\mathbf{n}^2 \to 1$. We can now use the Lagrangian corresponding to the Hamiltonian (8.4) to write the action S in Euclidean space (coordinate x + imaginary time τ) in the form

$$S = \frac{1}{2g}\int dx \int_{_j} d\tau [(\dot{n})^2 + (\nabla n)^2] + i\theta Q, \tag{8.5}$$

where

$$Q = \frac{1}{4\pi}\int (\mathbf{n}\,[\partial_x \mathbf{n} \partial_\tau \mathbf{n}])\, dx d\tau \tag{8.6}$$

is the topological charge. In our two-dimensional Euclidean space, the topological charge is a topological invariant that assumes integral values.

It is well known that the amplitude for the transition of a particle from one point in space-time to another is described by a functional integral over the trajectory, the weight of each trajectory being determined by the action. In Euclidean space, this weight is proportional to $\exp(-S/\hbar)$, which readily shows the difference between the contributions of the topological term in (8.5) for systems with integral and half-integrals spins. Actually, for integral spins (in the limit of large S), the contribution of the topological term to $\exp(-S/\hbar)$ does not differ from $(+1)$. Consequently, in this case, we can put $\theta = 0$. Conversely, for half-integral spins, this contribution is $(-1)^Q = (\pm 1)$, depending on the parity of the topological charge. In this case, $\theta = \pi$. Therefore, for systems with half-integral spins, the topological terms leads to "quantum interference" of topologically different trajectories $\mathbf{n}(x,\tau)$ in the functional integral for the transition amplitude.

Let us now examine the question of long range order in the ground state of the antiferromagnetic chain consisting of integral spins. We note, to start with, that the action given by (8.5) coincides for $\theta = 0$, with the functional limit of $\mathscr{H}/kT$, i.e. the effective Hamiltonian for the classical Heisenberg two-dimensional ferromagnet with effective temperature g. To this we add the point that the partition function $Z = \mathrm{Tr}\exp(-\mathscr{H}/kT)$ can also be written as the functional integral with respect to the "field" $\mathbf{n}(x_1, x_2)$ with weight $\exp(-\mathscr{H}/kT)$ (we have put $\tau \equiv x_2$). The problem of the long range order of the antiferromagnetic chain in which we are interested here can therefore be solved with the aid of the two-dimensional classical ferromagnet. According to the theorem of Mermin and Wagner, long range order arises in the two-dimensional model only for $T = 0$, so that the correlation length is finite for $T \neq 0$ and, as shown in Ref. 47, it increases exponentially as $T \to 0$. Bearing in mind that, in this case, the quantity g plays the part of temperature, we immediately see that the correlation length is finite in the ground state of the antiferromagnet, and, according to Ref. 47, takes the form

$$\xi \approx e^{2\pi/g}. \tag{8.7}$$

This correlation length corresponds to the gap

$$\Delta \sim \xi^{-1} \approx e^{-2\pi/g}. \tag{8.8}$$

in the excitation spectrum. The ground state of the antiferromagnetic chain consisting of integral spin is therefore disordered, nondegenerate, and has a gap in its excitation spectrum.

Once we have the results for the one-dimensional antiferromagnet, we can try to answer the following question: is there a topological term in the action for the two-dimensional antiferromagnet? This is a topical question because of the RVB theory in which there are neutral Fermi excitations with spin half (spinons). Attempts have recently been made to gain an understanding of the nature of these neutral fermions in terms of field-theoretic ideas. The basis for this was Ref. 84 in which it was noted that nonlinear excitations (skyrmions) arising in the nonlinear $(2+1)$-dimensional σ-model have spin that can be determined by eliminating the topological term from the action. For the nonlinear $(2+1)$-dimensional σ-model with the field $\mathbf{n}(x,y,t)$, the topological invariant is the Hopf invariant H, and the topologically different trajectories are classified by the Hopf index (an integral). By analogy with (8.5), we can now write down the expression for the action that corresponds to the field $\mathbf{n}(x,y,\tau)$ in euclidean space:

$$S = \frac{1}{2g}\int\int [(\dot{n})^2 + (\nabla n)^2]\, dr d\tau + i\theta H. \tag{8.9}$$

The Hopf invariant takes the form of a complicated integral of an expression that consists of the components of the vector $\mathbf{n}$ and its derivatives. Hence, by virtue of homotopy theory, it is the coupling coefficient between curves in the space (x,y,τ).[85] The authors of Refs. 86 and 87 assumed that neutral fermions with spin half, i.e., the spinons of RVB theory, were none other than the skyrmions, i.e., the topological excitations of the $(2+1)$-dimensional nonlinear σ-model, where the σ-model with the Hopf invariant in the action describes the two-dimensional quantum antiferromagnet.

Considerable effort[88,92] has been expended in trying to obtain the action from the microscopic model as a way of elucidating the situation. It was eventually found that the topological Hopf invariant in the action for the two-dimensional quantum Heisenberg antiferromagnet with nearest-neighbor interaction does not appear, so that skyrmions cannot have half-integral spin. A recent critical evaluation of the situation[110] concludes that the absence of the topological Hopf invariant in the action is due to the fact that the discussion in Refs. 88–92 was confined to the Néel ground state. If on the other hand, one were to consider other states, for example, the "current phase" obtained in Refs. 65 and 70 for the generalized current phase of Ref. 86b, then one would hope[88-92] to show that the topological invariant will appear in a self-consistent manner in the action.

We now return to the question of long range order in two-dimensional Heisenberg antiferromagnets. The g, T phase diagram can be investigated by the renormalization group method[93] for the system whose action is given by (8.9), but without the topological term

$$\frac{1}{\hbar}S = \frac{1}{2\tilde{g}}\int_0^{\beta\hbar c\Lambda} d\tau \int dr\, [(\dot{n})^2 + (\nabla n)^2] \tag{8.10}$$

where $\tilde{g} = \hbar c\Lambda/JS^2\alpha$, Λ is the maximum wave vector, α defines the degree of frustration of the lattice ($\alpha = 0$ for total frustration), c is the velocity of spin waves, and $\beta = 1/kT$. The renormalization group equations for the coupling constant g show that, for $T = 0$, there is a nontrivial fixed point $\tilde{g}_c = 4\pi$ that describes the quantum phase transition with the critical indices of the classical three-dimensional Heisen-

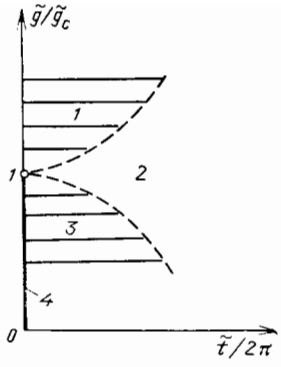

FIG. 28. Phase diagram for the two-dimensional Heisenberg model in terms of the variables $\tilde{g}$ and $\tilde{t}$ (Refs. 93): 1—disordered quantum region, 2—critical quantum region, 3—renormalized classical region, 4—Néel state.

berg model. The phase diagram on the $(\tilde{g}, \tilde{t})$ plane,is shown in Fig. 28. Thus, when $T=0$, the Néel order exists for coupling constants $\tilde{g}<\tilde{g}_c$, and an disordered quantum phase with excitation gap (quantum paramagnet) arises for $\tilde{g}>\tilde{g}_c$. We emphasize that an increasing $\tilde{g}$ corresponds to small S and α.

We shall now reproduce the correlation length calculations for different regions on the phase diagram. In the renormalized classical region (for $\tilde{g}<\tilde{g}_c$), the correlation length diverges exponentially as $T\to 0$:

$$\xi \approx 0.9\frac{\hbar c}{kT}\exp\left[\frac{2\pi}{kT}\left(1-\frac{\tilde{g}}{\tilde{g}_c}\right)JS^2\right]. \tag{8.11}$$

In the disordered quantum region $(\tilde{g}>\tilde{g}_c)$, the correlation length becomes independent of temperature as $T\to 0$, and is given by

$$\xi(T=0)\approx\left(\frac{\tilde{g}}{\tilde{g}_c}-1\right)^{-\nu}, \tag{8.12}$$

where ν is found to be equal to 1, Finally, for $\tilde{g}=\tilde{g}_c$, it is found that

$$\xi(T)\approx\frac{\hbar c}{kT}. \tag{8.13}$$

Figure 28 shows the crossover lines between different regimes. The expression for the line with $\tilde{g}>\tilde{g}_c$, which separates regions 1 and 2, can be estimated from

$$T_x\sim\frac{\Delta}{k}\sim\left(\frac{\tilde{g}}{\tilde{g}_c}-1\right)^{\nu}.$$

For $\tilde{g}<\tilde{g}_c$, the crossover line separating regions 2 and 3 is given by

$$T_x'\sim\left(1-\frac{\tilde{g}}{\tilde{g}_c}\right)^{\nu}.$$

Let us now return to the inelastic scattering of neutrons by La_2CuO_4. The question is: what is the range of values of the coupling constant g for this compound? The presence or otherwise of long range order cannot be established because the onset of the observed three-dimensional order is due to the interaction between the planes. However, the tempera ture dependence of the correlation length (cf. Fig. 18) suggests that $\tilde{g}<\tilde{g}_c$ in La_2CuO_4. The theoretical curve based on (8.11) is superimposed on the experimental points of Fig. 18 for the following parameter values: $\tilde{g}/\tilde{g}_c\equiv 0.685$, $\hbar c = 0.425$ eV Å, and is in agreement with the inelastic scattering data given in Sec. 6. Judging by this comparison between theory and experiment, the compound La_2CuO_4 is in the state of renormalized classical critical fluctuation of the Néel order parameter for $T>T_N$.

A possible explanation of the unusual spin correlations in La_2CuO_4 at temperatures above T_N may therefore be found in the relatively strong quantum fluctuations, typical for this compound, as indicated by the experimental data of Sec. 6. We know that classical fluctuations play an important part in the two-dimensional case. Polyakov[47] has shown that they lead to a exponential dependence of the correlation length on temperature. In the quantum antiferromagnet, quantum effects produce a renormalization of the correlation length of classical fluctuations. In particular, the exponential dependence of the correlation length on temperature for $\tilde{g}<\tilde{g}_c$ is retained [cf (8.11)], but the correlation length is reduced as compared with the classical result. Comparison between theory and experimental results shows that this situation occurs in La_2CuO_4. With increasing frustration produced by doping, the coupling constant $\tilde{g}$ is found to increase and, when $\tilde{g}>\tilde{g}_c$ $(T=0)$, the disordered quantum phase arises with a gap in the excitation spectrum. According to Ref. 93, this phase is similar to the RVB state in the version proposed in Ref. 62. On the other hand, if it is found that $\tilde{g}=\tilde{g}_c$, then the $(T=0)$-spectrum of the excitations will become gapless, and the resulting phase will resemble the RVB state in Anderson's formulation.

9. *Superconductivity due to magnetic degrees of freedom in systems with weak Coulomb interaction.* The discovery of high-temperature superconductivity has not only stimulated the development of interpretations, e.g., the RVB theory, but has also triggered renewed interest in existing theories. This applies, in the first instance, to theories that take into account specific properties of the Fermi surface of metals. One of them is the presence of flat areas on the Fermi surface that coincide with one another when they are displaced by a wave vector $\mathbf{Q}$ (nesting). This can lead to pairing interactions between electrons via the magnetic degrees of freedom. Although this mechanism does not provide a complete description of superconductivity in HTSCs, studies of it have led to extensive and useful material that will have to be taken into account when a complete theory of high-temperature superconductivity eventually emerges.

We begin with the three-dimensional cubic crystal described by the Hubbard model and having a "bare" electron spectrum of the form

$$E_{\mathbf{k}} = -2t(\cos k_x + \cos k_y + \cos k_z). \tag{9.1}$$

We know that, in the random-phase approximation, the spin susceptibility $\chi(\mathbf{q})$ has a pole at the point $\mathbf{q}=\mathbf{Q}$ (the vector $\mathbf{Q}$ is defined below):

$$1 - U\chi_0(\mathbf{Q}_0), \tag{9.2}$$

which corresponds to a ground-state instability with the formation of a spin density wave, where $\chi_0(\mathbf{q})$ is the free-electron susceptibility

$$\chi_0(\mathbf{q}) = \sum_{\mathbf{k}}\frac{f(\varepsilon_{\mathbf{k}+\mathbf{q}})-f(\varepsilon_{\mathbf{k}})}{\varepsilon_{\mathbf{k}}-\varepsilon_{\mathbf{k}+\mathbf{q}}}, \tag{9.3}$$

$f(\varepsilon)$ is the Fermi function, and $\varepsilon_{\mathbf{k}} = E_{\mathbf{k}} - \mu$.

For a half-filled band ($\mu = 0$), the Fermi surface has the ideal nesting for ($\mathbf{Q} = (\pm\pi, \pm\pi, \pm\pi)$: $\varepsilon_{\mathbf{k}+\mathbf{Q}} = -\varepsilon_{\mathbf{k}}$. When $\mathbf{q} = \mathbf{Q}$ and $\mu = 0$, we have the following estimate for $\chi_0(\mathbf{q})$:

$$\chi_0(\mathbf{Q}) \sim \ln \frac{t}{T}, \tag{9.4}$$

so that, for all values of U, the condition (9.2) is always satisfied for finite T. When $\mu \neq 0$ and $T = 0$, we have

$$\chi_0(\mathbf{Q}) \sim \ln \frac{t}{\mu}. \tag{9.5}$$

For fixed U and with (9.2) satisfied, there then exists a critical value of μ for which

$$1 = U\chi_0(\mathbf{Q}, \mu_c, T = 0). \tag{9.6}$$

We shall be interested in the case $\mu < \mu_c$, and will determine the corresponding superconducting transition point due to the inclusion of the pairing mechanism for electrons via the fluctuations of the state with the spin density wave in the pretransition regime, i.e., when the transition to the state with the spin density wave has not yet taken place.[94] We shall assume that the superconducting transition occurs at low enough temperatures, so that χ_0 is close to its value for $T = 0$, and we can use (9.6).

The pairing interaction between electrons in the singlet and triplet channels is obtained by summing graphs with an antiparallel ladder and simple electron loops. This leads to[94]

$$V_s(\mathbf{k}, \mathbf{k}') = U + \frac{U^3\chi_0^2(\mathbf{k}' - \mathbf{k})}{1 - U^2\chi_0^2(\mathbf{k}' - \mathbf{k})} + \frac{U^2\chi_0(\mathbf{k}' + \mathbf{k})}{1 - U\chi_0(\mathbf{k}' + \mathbf{k})}, \tag{9.7}$$

$$V_t(\mathbf{k}, \mathbf{k}') = -\frac{U^2\chi_0(\mathbf{k}' - \mathbf{k})}{1 - U^2\chi_0^2(\mathbf{k}' - \mathbf{k})}. \tag{9.8}$$

To evaluate T_c, we use the well known formulas for superconductors with strong coupling (cf., for example, Ref. 95) in which the coupling constant is given by

$$\lambda = 2\int_0^\infty \frac{F(\omega)}{\omega} d\omega, \quad F(\omega) = \left\langle -\frac{1}{\pi} \operatorname{Im} V(\mathbf{k}, \mathbf{k}', \omega) \right\rangle_F, \tag{9.9}$$

where $V(\mathbf{k}, \mathbf{k}', \omega)$ is the effective interaction between electrons on the Fermi surface and the symbol $\langle \ldots \rangle_F$ represents averaging over this surface. If we are interested in the partial contribution to λ due to states of a Cooper pair with given orbital angular momentum l, and use the dispersion relations (9.9) we can write

$$\lambda_l = -\langle f_l(\mathbf{k}) \operatorname{Re} V(\mathbf{k}, \mathbf{k}', 0) f_l(\mathbf{k}') \rangle_F; \tag{9.10}$$

where $f_l(\mathbf{k})$ are the basic functions for the orbital state in the crystal field.

The coupling constant λ_l (subject to $\lambda_l > 0$) determines the transition temperature for the superconducting state with l-type pairing, where

$$T_{cl} = \omega_c e^{-1/\lambda_l}, \tag{9.11}$$

in which ω_c is the cut-off energy (of the order of the maximum energy of spin fluctuations that mediate the pairing interaction).

The basis functions $f_l(\mathbf{k})$ should be taken in the strong-coupling approximation. For states with s, p, and d-symmetry in a cubic crystal, they are

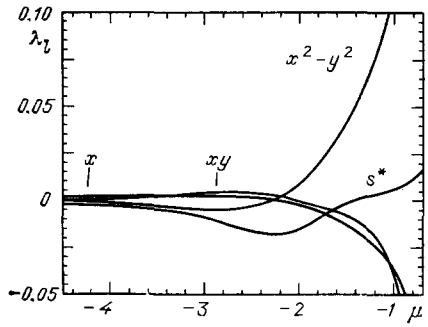

FIG. 29. The coupling constant λ_l as a function of μ for $U = 4$, $\mu_c = -0.71$ (Ref. 94). The quantities U and μ are expressed in units of t.

$$\begin{aligned} &\text{s:} && \cos k_x + \cos k_y + \cos k_z, \\ &\text{p:} && \sin k_x,\ \sin k_y,\ \sin k_z, \\ &\text{d}(e_g): && \cos k_x - \cos k_y,\quad 2\cos k_z - \cos k_x - \cos k_y, \\ &\text{d}(t_{2g}): && \sin k_x \sin k_y,\quad \sin k_x \sin k_z,\quad \sin k_y \sin k_z. \end{aligned} \tag{9.12}$$

The expressions given by (9.7)–(9.12) were used in Ref. 94 to calculate the constants λ_l as functions of μ for different values of the Coulomb repulsion U. The graph of $\lambda_l(\mu)$ is shown in Fig. 29. It is clear that, as the chemical potential μ increases toward its critical value μ_c, the dominant coupling constant λ_l corresponds to a $d(e_g)$-type state (of course, for singlet pairing). The coupling constant is too small for this mechanism to explain high-temperature superconductivity.

Nevertheless, we now turn to the two-dimensional case near the half-filled state. The electron spectrum is shown in Fig. 11. If the half-filling is exact, the Fermi surface touches the boundary of the Brillouin zone at A, B, C, and D, and the neighborhoods of these points provide a singular contribution to the density of states

$$N(\varepsilon) \sim \ln \varepsilon \tag{9.13}$$

(van Hove singularity). Let us consider the contribution of electron states near this singularity to superconductivity.[96] Whatever the electron pairing mechanism, T_c is given by the following equation in weak-coupling theory:

$$1 = \lambda \int_0^{\omega_c} N(\varepsilon) \operatorname{th} \frac{\varepsilon}{2kT_c} \varepsilon^{-1} d\varepsilon \sim \lambda \ln^2 \frac{\omega_c}{kT_c}, \tag{9.14}$$

so that

$$T_c \sim \omega_c \exp\left(-\frac{1}{\lambda^{1/2}}\right) \tag{9.15}$$

which differs from (9.11). Hence, for small $\lambda < 1$, the singularity of $N(\varepsilon)$ leads to a higher T_c.

The contribution of van Hove singularities to T_c must now be evaluated in greater detail. Simple analysis[97] shows that, near A, B, C, and D (Fig. 11), both the Cooper channel that corresponds to the interaction of electrons from A and C, and the zero-sound channel, in which electrons from A and B interact, are "doubly logarithmic" [cf. (9.14)]. In this situation, we must sum all diagrams that are of the same order of magnitude in the double-logarithmic approxima-

tion, $\lambda \ln^2(\omega_c/\varepsilon) \sim 1$. These are the so-called parquet diagrams. A very laborious and complicated method of evaluating the vertex parts and response functions is described in detail in Ref. 97. It has produced the singular parts in terms of response functions, namely, the response χ_{ss} to singlet superconductivity, the response χ_{SDW} to the spontaneous spin density waves, and the response χ_{CDW} to the charge density waves. The solutions obtained for the response functions include solutions that give independent singlet superconductivity, spin density wave, and charge density wave. However, there is also a solution that corresponds to a possible transition to a state that is a coherent combination of superconductivity, antiferromagnetism, and a charge density wave.

Although, this result is unlikely to be useful in the explanation of the HTSC mechanism, it provides an example of an interesting and very complicated theoretical problem in physics, which has arisen in connection with the HTSC problem.

A further mechanism of electron pairing has recently been proposed and is based on the existence of antiferromagnetism.[98-100] By analogy with the "bag" model in quantum chromodynamics, it is referred to as the "spin-bag theory". Let us turn once again to the three-dimensional Hubbard model with weak Coulomb interaction $U \lesssim t$. Because of nesting, we then have a spin density wave with wave vector $\mathbf{Q} = (\pi,\pi)$, which is responsible for the opening up of a gap $2\Delta_{SDW}$ on the Fermi surface.

Let us now consider what can happen if we add an electron hole to this state.

The result of this is an effect similar to the spin polaron. The addition of the hole reduces the electron charge density and thus reduces the magnetic order parameter $\mathbf{m}$ at the given point. Since the local value of the energy gap $\Delta_{SDW}(x)$ is proportional to $\mathbf{m}(x)$, it follows that the hole will suppress the gap in its neighborhood. The energy of the hole will be reduced in this region. The hole is thus seen to give rise to an effective potential well or "bag" in its neighborhood, and is itself trapped by this bag. The hole and its surrounding bag move through the crystal, and together behave as a Fermi particle of charge e^+ and spin 1/2. When two such particles interact, the effective potential due to the "unified bag" can be attractive. According to Ref. 98, this attraction is the interaction that is responsible for superconducting properties.

The problem now is to cast the physical picture into a mathematical form. Unfortunately, the situation is not as favorable as it might appear at first sight. The authors of Ref. 98 have shown that the superconducting gap is given by

$$\Delta_{SC} \approx \Delta_{SDW} e^{-t/\alpha U},$$

where α is a constant of the order of unity. On the other hand, serious objections were raised in Ref. 99 against the validity of the effective interaction (Ref. 98) but, despite these objections, there is no doubt that this type of pairing interaction can actually occur. However, to demonstrate the attractive character of the interaction, we need a more detailed microscopic theory of the phenomenon and, so far, the question remains an open one.

10. *Conclusion.* Of the four known classes of copper oxide HTSCs, only two, namely, $La_{2-x}Sr_xCuO_4$ and $YBa_2Cu_3O_{7-\delta}$, have been investigated in the necessary detail from the point of view of the magnetic properties. It is remarkable that these systems exhibit similar behavior as x and δ are varied. Near the stoichiometric composition ($x \approx 0$ or $\delta \approx 1$, the two systems exhibit the same type of antiferromagnetic ordering in the copper sublattice with comparable values of T_N that fall rapidly with increasing x and δ, i.e., with increasing carrier concentration. Outside the interval in which there is long range antiferromagnetic order, the spin glass phase arises at low temperatures.

The magnetic moment of a copper atom is $\sim 0.5\mu_B$ and is independent of carrier concentration. Recent experiments have revealed the same type of antiferromagnetic order in the CuO_2 planes of Bi and Tl compounds.

Studies of spin dynamics in the La and Y–Ba systems have also demonstrated their similarity. For example, both systems probably contain quasi-two-dimensional magnetic fluctuations which, at about 100° above T_N have a correlation length of the order of 100 Å. These fluctuations have high energies, and their velocity is of the order of 0.5 eV Å. More detailed studies of La_2CuO_4 show that it offers a good realization of the two-dimensional Heisenberg quantum antiferromagnet with spin 1/2. Long range magnetic order rapidly disappears with increasing dopant concentration, but the system becomes a "quantum spin fluid" characterized by long correlation lengths and high energy of spin excitations. Studies of the spin dynamics of other HTSCs have run into the serious problem of availability of high-grade single crystals.

The most interesting question is the connection between magnetic and superconducting ordering. In the La and Y–Ba systems, superconductivity appears for compositions for which there is no magnetic ordering, but there are exceptions to this rule. For example, in a recent paper.[101] neutron diffraction studies were said to have revealed the coexistence of antiferromagnetic order $T_N = 230$ K and superconductivity ($T_c = 55$ K) in single-crystal $YBa_2Cu_3O_{6.55}$. For other compositions, for which in the superconducting state there is no long range magnetic order, there is considerable interest in studies of magnetic fluctuations as possible conveyors of the pairing interaction. The importance of magnetic fluctuations in the subsystem of $3d$-electrons of copper, and the participation of the latter in the superconducting transition, are clearly shown by NMR experiments (see, for example, Ref. 102).

Experimental studies of the magnetic properties of the copper oxides have triggered the development of a number of new areas in condensed state theory, e.g., the two-dimensional Heisenberg model with $S = 1/2$, the nonlinear σ-model, and the Hubbard model. For example, the theory of resonating valence bonds in the two-dimensional Hubbard model with its neutral fermions and charged bosons has grown out of experimental studies of the magnetic properties of HTSCs. It is still too early to speak of a comparison between the conclusions of this theory and experiment, especially since the theory itself is incomplete. However, whether or not all these ideas will be important for the explanation of high-temperature superconductivity, they will probably remain in the arsenal of the theory of low-dimensional systems.

The experimental data that have now accumulated pose

the serious question of whether there is a connection between magnetism and superconductivity in copper oxide HTSCs. The question has not been answered, but there are still hopes that magnetism will be fundamental to high-temperature superconductivity. However, the discovery of the (K, Ba)BiO_3 compound with perovskite structure and $T_c = 30$ K, which does not contain copper and does not therefore have atomic magnetic moments, has again brought to the fore the electron-phonon mechanism. It is likely that the phonon mechanism contributes to T_c, but we do not know which particular phonon mechanism it is. This is indicated by the strong coupling effects in the Y–Ba system (see, for example, Ref. 103). Structural instability and its possible influence on HTSCs is again attracting considerable interest to the HTSCs problem. They are reviewed in detail in Ref. 104. Whatever the final solution of the problem of superconducting pairing in HTSCs, the development of a systematic theory of this phenomenon will undoubtedly involve the inclusion of strong Coulomb correlations in the system of $3d$-electrons of copper and their associated spin correlations.

A multiplicity of new results has recently appeared in the theory of the Heisenberg model of the two-dimensional frustrated quantum antiferromagnet with spin 1/2. In particular, it has been shown that the ground state of this model is a chiral spin fluid, and that the elementary excitations above it obey fractional statistics. These and other questions relating to the possibility of superconductivity in a particle gas with fractional statistics are discussed in detail in a recent review paper[111] which lists the most recent references.

[1)] The compounds $Nd_{2-x}Ce_xCuO_4$ were recently synthesized[105] (with electrons as carriers).

[1] L. P. Gor'kov and N. B. Kopnin, Usp. Fiz. Nauk. **156**, 117 (1988) [Sov. Phys. Usp. **31**, 850 (1988)].
[2] L. N. Bulaevskii, V. L. Ginzburg, and A. A. Sobyanin, Zh. Eksp. Teor. Fiz. **94**, 355 (1988) [Sov. Phys. JETP **67**, 1499 (1988)].
[3] J. D. Jorgensen, H. -B. Schuttler, D. G. Hinks, D. W. Capone, K. Zhang, M. B. Brodsky, and D. J. Scalapino, Phys. Rev. Lett. **58**, 1024 (1987).
[4] P. Boni, J. D. Axe, G. Shirane, R. J. Birgeneau, D. R. Gabbe, H. Henssen, M. A. Kastner, C. J. Peters, P. J. Picone, and T. R. Thurston, Phys. Rev. B **38**, 185 (1988).
[5] J. D. Jorgenson, B. Veal, W. K. Kwok, G. W. Crabtree, A. Umezawa, L. J. Nowicki, and A. P. Paulikas, *ibid.* **36**, 5731 (1987).
[6] M. Francois, A. Junod, K. Yvon, P. Fischer, J. J. Capponi, P. Strobel, M. Marezio, and A. W. Hewat, Solid State Commun. **66**, 1117 (1988).
[7] Yu. A. Izyumov and M. I. Kitzmel'son, Fiz. Met. Metalloved. **66**, 1083 (1988) [Phys. Met. Metallogr. **66**, in press (1988)].
[8] K. Zhang, B. Dabrowskii, C. U. Segre, D. G. Hinks, I. K. Schuller, J. D. Jorgensen, and M. Slaski, Preprint ANL, 1988; J. Phys. C (to be published).
[9] Yu. A. Osipyan, V. Sh. Shekhtman, and I. M. Shmyt'koo, Physica C **153–155**, 970 (1988).
[10] K. L. Hodeau, P. Bordet, J. J. Capponi, C. Chaillout and M. Maresio, *ibid.* p. 582.
[11] S. A. Sunshine, T. Siegrist, L. F. Schneemeyer, D. W. Murphy, R. J. Cava, B. Batlogg, R. B. van Dover, R. M. Fleming, S. H. Glarum, S. Nakahara, R. Farrow, J. J. Krajewski, S. M. Zahurak, J. Waszczak, J. H. Marshall, P. Marsh, L. W. Rupp, Jr., and W. F. Peck, Phys. Rev. B **38**, 893 (1988).
[12] J. M. Tarascon, Y. Le Page, P. Barboux, B. G. Bagley, L. Greene, W. R. McKinnon, G. W. Hull, M. Giroud, and D. M. Hwang, *ibid.* **37**, 9382.
[13] J. M. Tranquada, A. H. Moudden, A. I. Goldman, P. Zolliker, D. E. Cox, G. Shirane, S. K. Sinha, D. Vaknin, D. C. Johnson, M. S. Alvarez, A. J. Jacobson, J. T. Lewandowski, and J. M. Newsam, *ibid.* **38**, 2477.
[14] G. Xiao, F. H. Streitz, A. Gavrin, Y. W. Du, and C. L. Chien, *ibid.* **35**, 8782 (1987).
[15] G. Xiao, M. Z. Cieplak, A. Gavrin, F. H. Streitz, A. Bakhshai, and C. L. Chien, Phys. Rev. Lett. **60**, 1446 (1988).
[16] D. I. Khomskiĭ, Proc. Internat. Conf. on Mechanisms of High T_c Superconductivity [in Russian], JINR, Dubna, 1988, p. 135.
[17] N. F. Mott, Metal-Insulator Transitions, Taylor and Francis, London, 1974. [Russ. transl., Nauka, M., 1979]. P. W. Anderson, 50 years of the Mott phenomenon. Lecture given at Varenna Summer School on Frontiers and Borderlines in Many - Particle Physics, July, 1987.
[18] N. Nücker, J. Fink, J. C. Fuggle, P. J. Durham, and W. M. Temmerman, Physica C **153–155**, 119 (1988).
[19] L. F. Matheis, Phys. Rev. Lett. **58**, 1028 (1987).
[20] A. J. Freeman, J. Yu, and C. L. Fu, Phys. Rev. B **36**, 7111 (1987).
[21] J. H. Xu, T. J. Watson-Yang, J. Yu, and A. J. Freeman, Phys. Lett. A**120**, 489 (1987).
[22] S. Massida, J. Yu, and A. J. Freeman, *ibid.*, **122**, 148.
[23] A. J. Freeman, Physica, C **153–155**, 1225 (1988).
[24] J. Yu, S. Massida, and A. J. Freeman, *ibid.*, **152**, 273.
[25] J. Zaanen, O. Jepson, O. Gunnarsson, A. T. Paxton, and O. K. Andersen, *ibid.* **153–155**, 1636.
[26] V. I. Anisimov, M. A. Korotin, and I. V. Afanasyev, *ibid.* **159**, 412 (1989).
[27] R. J. Birgeneau and G. Shirane, Physical Properties of High Temperature Superconductors, ed. D. M. Ginsberg, World Scientific, Singapore, 1989.
[28] D. Vaknin, S. K. Sinha, D. E. Moncton, and D. C. Johnston, J. Newsam, C. R. Safinya, and H. E. King Jr., Phys. Rev. Lett. **58**, 2802 (1987).
[29] D. C. Johnson, S. K. Sinham, A. J. Jacobson, and J. M. Newsam, Physica C **153–155**, 572 (1988).
[30] M. A. Kastner, R. J. Birgeneau, T. R. Thurston, H. P. Jenssen, D. R. Gabbe, M. Sato, K. Fukuda, S. Shanuto, Y. Endoh, K. Yamada, and G. Shirane, Phys. Rev. B **38**, 6636 (1988).
[31] A. S. Borovik-Romanov, A. I. Buzdin, N. M. Kreĭnes, and S. S. Krotov, Pis'ma Zh. Eksp. Teor. Fiz. **47**, 600 (1988) [JETP Lett. **47**, 697 (1988)].
[32] N. M. Plakida, Iz. Akad. Nauk. SSSR Ser. Fiz. **53**, 1236 (1989) [Bull. Acad. Sci. USSR Phys. Ser. **53** (1989)].
[33] A. Aharony, R. T. Birgeneau, A. Coniglio, M. A. Kastner, and H. E. Stanley, Phys. Rev. Lett. **60**, 1330 (1988).
[34] J. M. Tranquada, A. H. Moudden, A. I. Goldman, P. Zolliker, M. S. Varez, A. J. Jacobson, J. T. Lewandowski and J. M. Newsam, Phys. Rev. B**38**, 2477 (1988).
[35] H. Kradowaki, M. Hishi, Y. Yamada, H. Takeya, H. Takei, S. Shapiro and G. Shirance, *ibid.*, **37**, 7932.
[36] J. H. Brewer, E. J. Ansaldo, J. F. Carolan, *et al.*, Phys. Rev. Lett. **60**, 1073 (1988).
[37] J. Rossat-Mignod, P. Burlet, M. J. G. Jurgens, C. Vettier, L. P. Regnault, J. V. Henry, C. Ayache, L. Forro, H. Noel, M. Potel, P. Gougeon, and J. C. Levet, J. Phys. (Paris) **49**, C8-2119 (1988).
[38] A. P. Ramirez, L. F. Schneemeyer, and J. V. Waszczak, Phys. Rev. B **36**, 7145 (1987).
[39] J. W. Lynn, W. H. Li, N. A. Mook, B. C. Sales, and Z. Fisk, Phys. Rev. Lett. **60**, 2781 (1988).
[40] W. H. Li, J. W. Lynn, S. Skanthakumar, T. W. Clinton, A. Kebede, C. S. Lee, J. E. Crow, and T. Mihalisin, Preprint, 1989.
[41] T. Thio, T. R. Thurston, N. W. Preyer, P. J. Picone, M. A. Kastner, H. P. Jenssen, FD. R. Gabbe, C. Y. Chen, R. J. Birgeneau, A. Aharony, Phys. Rev. B **38**, 905 (1988).
[42] V. G. Baryahtar, V. M. Loktev, and D. A. Yablonskii, Physica C **156**, 667 (1988).
[43] G. Shirane, Y. Endoh Y, R. J. Birgeneau, M. A. Kastner, Y. Hidaka, M. Oda, M. Suzuki, and T. Murakami, Phys. Rev. Lett. **59**, 1613 (1987).
[44] Y. Endoh, K. Yamanda, R. J. Birgeneau, M. A. Kastner, Y. Hidaka, M. A. Kastner, C. J. Peters, P. J. Picone, T. R. Thurston, J. M. Tranquada, G. Shirane, Y. Hidaka, M. Oda, Y. Enomoto, M. Suzuki, and T. Murakami, Phys. Rev. B **37**, 7443 (1988).
[45] R. J. Birgeneau, D. R. Gabbe, H. P. Jenssen, M. A. Kastner, P. J. Picone, T. R. Thurston, G. Shirane, Y. Endoh, M. Sato, K. Yamada, Y. Hidaka, M. M. Oda, Y. Enomoto, M. Suzuki, and T. Murakami, *ibid.* **37**, 2353.
[46] K. B. Lyons, P. A. Fleury, J. P. Remeika, A. S. Cooper, and T. J. Negran, *ibid.* **38**, 6614.
[47] A. M. Polyakov, Phys. Lett. B**59**, 79 (1975).
[48a)] M. Sato, S. Shamoto, J. M. Tranquada, G. Shirane, and B. Keimer, Phys. Rev. Lett. **61**, 1317 (1988).
[48b)] J. M. Tranquada, G. Shirane, B. Keimer, S. Shamato, and M. Sato, Phys. Rev. Ser. B (1989).
[49] K. B. Lyons, P. A. Fleury, L. F. Schneemeyer, and J. V. Waszczak, Phys. Rev. Lett. **60**, 732 (1988).
[50] F. Mezei, B. Farago, C. Pappas, Gy. Hutiray, L. Roste, and L. Mihaly, Physica. C **153–155**, 1669 (1988).
[51] J. Mizuki, Y. Kobo, T. Manako, Y. Shimakawa, H. Igerashi, J. M. Tranquada, Y. Fujii, L. Rebelsky, and G. Shirane, *ibid.* **156**, 781.
[52] D. I. Khomskiĭ, Fiz. Met. Metalloved. **29**, 31 (1970) [Phys. Met. Metalogr. **29**, (1), 31 (1970)]
[53] E. H. Lieb and F. Y. Wu, Phys. Rev. Lett. **20**, 1445 (1968).

[54] Y. Nagaoka, Phys. Rev. **147**, 392 (1966).
[55] H. Shiba, *ibid.* B **6**, 930 (1972).
[56] P. W. Anderson, Phys. Rev. **147**, 392 (1966).
[57] Yu. A. Izyumov and Yu. N. Skryabin, Statistical Mechanics of Magnetically Ordered systems [in Russian], Nauka, M., 1987.
[58] L. A. Takhtajan, and L. D. Faddeev, Phys. Lett. **85**, 375 (1981).
[59] P. W. Anderson, Mater. Res. Bull. **8**, 153 (1973).
[60] P. W. Anderson, Science **235**, 1196 (1987).
[61] C. Gros, R. Joynt, and T. M. Rice, Phys. Rev. **B36**, 381 (1987).
[62] S. A. Kivelson, D. S. Rokhsar, and J. P. Sethna, *ibid.* **35**, 8865.
[63] S. A. Kivelson, *ibid.* **36**, 7237.
[64] G. Baskaran, Z. Zou, and P. W. Anderson, Solid State Commun. **63**, 973 (1987).
[65] G. Kotliar, Phys. Rev. **B37**, 3664 (1988).
[66] I. Affleck, Z. Zou, T. Hsu, and P. W. Anderson, *ibid.* **38**, 745.
[67] P. W. Anderson, G. Baskaran, Z. Zou, and T. Hsu, Phys. Rev. Lett. **58**, 2790 (1987).
[68] P. W. Anderson, Problems and Issues in the RVB Theory of High-T_c Superconductivity, Cargese, May 1988, Lectures XI, Preprint, Princeton University.
[69] Z. Zou, and P. W. Anderson, Phys. Rev. **B37**, 627 (1988).
[70] I. Affleck and J. B. Marston, *ibid.* 3774.
[71] G. Baskaran, Internat. J. Mod. Phys. **1**, 539 (1988).
[72] H. Yokoyama, and H. Shiba, J. Phys. Soc. Jpn. **56**, 3570 (1987).
[73] J. Bonca, P. Preovsek, and I. Sega, Europhys. Lett. **10**, 87 (1989).
[74] F. C. Zhang, C. Gros, T. M. Rice, and H. Dhiba, Supercond. Sci. and Technol. **1**, 36 (1989).
[75] B. L. Ioffe, and A. I. Larkin, Phys. Rev. B, **37**, 3759 (1988).
[76] N. M. Plakida, V. Yu. Yushankhai, and I. V. Stasyuk, Physica C **160**, 80 (1989).
[77] V. J. Emery, Phys. Rev. Lett. **58**, 2794 (1987).
[78] F. C. Zhang, and T. M. Rice, Phys. Rev. B **37**, 3759 (1988).
[79] E. Lieb, T. Schultz and D. Mattis, Ann. Phys. (N.Y.) **16**, 407 (1961).
[80] F. D. M. Haldane, Phys. Lett. **93**, 464 (1983).
[81] I. Affleck, Phys. Rev. **B37**, 5186 (1988).
[82] F. D. M. Haldane, Phys. Lett. **50**, 1153 (1983).
[83] I. Affleck, Nucl. Phys. **B257**, 397 (1985).
[84] F. Wilczek, and A. Zee, Phys. Rev. Lett. **51**, 2250 (1983).
[85] I. E. Dzyaloshinskii, Pis'ma Zh. Eksp. Teor. Fiz. **47**, 650 (1988) [JETP Lett. **47**, 750 (1988)].
[86] P. B. Wiegmann, Phys. Rev. Lett. **60**, 821 (1988), Physica C **153–155**, 103 (1988).
[87] I. Dzyaloshinski, A. Polyakov, and P. Wiegmann, Phys. Lett. A **127**, 112 (1988).
[88] Z. G. Wen, and A. Zee, Phys. Rev. Lett. **61**, 1025 (1988).
[89] F. D. M. Haldane, *ibid.* p. 1029.
[90] T. Dombre and N. Read, Phys. Ser. **B38**, 7181 (1988).
[91] E. Fradkin and M. Stone, *ibid.* p. 7215.
[92] L. B. Ioffe and A. I. Larkin, Internat. J. Mod. Phys. **B2**, 203 (1988).
[93] S. Chakravarty, B. I. Halperin, and D. R. Nelson, Phys. Rev. Lett. **60**, 1057 (1988).
[94] D. J. Scalapino, E. Loh, and J. E. Hirsch, Phys. Rev. **B35**, 6694 (1987).
[95] S. V. Vonsovsky, Yu. A. Izyumov, and E. Z. Kurmaev, Superconductivity of Transition Metals, Their Alloys, and Compounds Springer-Verlag, Berlin 1982. [Russ. original, Nauka, M., 1977].
[96] J. E. Hirsch, and D. J. Scalapino, Phys. Rev. Lett. **60**, 944 (1988).
[97] I. E. Dzyaloshinskii, Zh. Eksp. Teor. Fiz. **93**, 1487 (1987) [Sov. Phys. JETP **66**, 848 (1987)].
[98] J. R. Schrieffer, X. G. Wen, and S. C. Zhang, Phys. Rev. Lett. **60**, 944 (1988).
[99] E. W. Fenton, Solid State. Commun. **67**, 1059 (1988).
[100] J. R. Schrieffer, X. G. Zen, and S. C. Zhang, Mod. Phys. Lett. **B2**, 935 (1988).
[101] D. Petitgrand, G. Collin, P. Schweiss, S. Hadjoudi, and S. Senoussi, J. Phys. (Paris) **49**, 1815 (1988).
[102] M. Horvatic, P. Segranson, C. Berthier *et al.*, Phys. Rev. B **39**, 10 (1989).
[103] L. N. Bulaevskii, O. V. Dolgov, I. P. Kazakov, S. N. Maksimovskii, M. O. Ptitsyn, V. A. Stepanov, and S. I. Vedeneev, Supercond. Sci. Technol. **1**, 205 (1988).
[104] N. M. Plakida, Phys. Scr. **29**, 8 (1989).
[105] Y. Tokura, H. Takagi, and S. Uchida, Nature **337**, 345 (1989).
[106] G. Shirane, Proceedings of an International Seminar on HTSC, Dubna, JINR, June 28–July 1, 1989.
[107] D. R. Harshman, G. Aeppli, G. P. Espinosa, S. A. Copper, J. P. Remeika, E. J. Ansaldi, T. M. Riseman, D. Li. Williams, D. R. Noakes, B. Ellman and T. F. Rosenbaum, Phys. Rev. **B38**, 852 (1988).
[108] V. J. Emery, and G. Reimer, *ibid.* p. 11938.
[109] F. C. Zhang and T. M. Rice, On the Validity of the *t-J* model -Preprint Hönggerberg, Switzerland, ETH, 1989 (Theoretische Physik).
[110] D. Khveshchenko and P. B. Wiegmann, Effective Action of Antiferromagnetism in Two-dimensions: Parity Violating Ground State and the Hall Effect, Preprint from the Landau Institute for Theoretical Physics, M., 1989.
[111] Y. H. Chen, F. Wilczek, E. Witten, and B. I. Halperin, Intern. J. Mod. Phys. **B3**, 1001 (1989).

Translated by S. Chomet